bioRxiv preprint doi: https://doi.org/10.1101/2021.12.08.471779; this version posted December 8, 2021. The copyright holder for this preprint (which was not certified by peer review) is the author/funder. All rights reserved. No reuse allowed without permission.

# Identification of New *In Vivo* TonB-FepA Rendezvous Sites

**Kathleen Postle[1, 2*], Kelvin Kho[1,3], Michael Gresock[1,4], Joydeep Ghosh[2, 5], and Ray Larsen[2,6]**

**Running title: *In vivo* TonB-FepA interactions**

**Keywords: TonB, FepA, disulfide bond, amphipathic helix, energy transduction**

**Department of Biochemistry and Molecular Biology, The Pennsylvania State University, University Park, PA, 16802, USA**

*** Correspondence: [1]Kathleen Postle, Department of Biochemistry and Molecular Biology, The Pennsylvania State University, University Park, PA 16802, USA. e-mail: postle@psu.edu, Ph. 1-814-863-7568, Fx. 1-814-863-7024**

bioRxiv preprint doi: https://doi.org/10.1101/2021.12.08.471779; this version posted December 8, 2021. The copyright holder for this preprint (which was not certified by peer review) is the author/funder. All rights reserved. No reuse allowed without permission.

**[2] School of Molecular Biosciences, Washington State University, Pullman, WA 99163**

**Current addresses:**

**[3]Institut Pasteur, Unité Biologie et Génétique de la Paroi Bactérienne, Département de Microbiologie, Paris 75015, France**

**[4]Department of Biology, University of Mt. Union, Alliance OH, 44601**

**[5]Division of Cellular and Gene Therapies, US FDA Center for Biologics Evaluation and Research, Silver Spring, MD**

**[5]Department of Biological Sciences, Bowling Green State University, Bowling Green OH, 43403**

bioRxiv preprint doi: https://doi.org/10.1101/2021.12.08.471779; this version posted December 8, 2021. The copyright holder for this preprint (which was not certified by peer review) is the author/funder. All rights reserved. No reuse allowed without permission.


## ABSTRACT

The TonB system of Gram-negative bacteria uses the protonmotive force of the cytoplasmic membrane to energize active transport of large or scarce nutrients across the outer membrane by means of customized beta-barrels known as TonB-dependent transporters (TBDTs). The lumen of each TBDT is occluded by an amino-terminal domain, called the cork, which must be displaced for transport of nutrients or translocation of the large protein toxins that parasitize the system. A complex of cytoplasmic membrane proteins consisting of TonB, ExbB and ExbD harnesses the protonmotive force that TonB transmits to the TBDT. The specifics of this energy transformation are a source of continuing interest. The amino terminal domain of a TBDT contains a region called the TonB box, that is essential for the reception of energy from TonB. This domain is the only identified site of *in vivo* interaction between the TBDT and TonB, occurring through a non-essential region centered on TonB residue Q160. Because TonB binds to TBDTs whether or not it is active or even intact, the mechanism and extent of cork movement *in vivo* has been challenging to discover. In this study, we used *in vivo* disulfide crosslinking between eight engineered Cys residues in *Escherichia coli* TonB and 42 Cys substitutions in the TBDT FepA, including the TonB box, to identify novel sites of interaction *in vivo*. The TonB Cys substitutions in the core of an essential carboxy terminal amphipathic helix (residues 199-216) were compared to TonB

bioRxiv preprint doi: https://doi.org/10.1101/2021.12.08.471779; this version posted December 8, 2021. The copyright holder for this preprint (which was not certified by peer review) is the author/funder. All rights reserved. No reuse allowed without permission.

Q160C interactions. Functionality of the *in vivo* interactions was established when the presence of the inactive TonB H20A mutation inhibited them. A previously unknown functional interaction between the hydrophilic face of the amphipathic helix and the FepA TonB box was identified. Interaction of Q160C with the FepA TonB box appeared to be less functionally important. The two different parts of TonB also differed in their interactions with the FepA cork and barrel turns. While the TonB amphipathic helix Cys residues interacted only with Cys residues on the periplasmic face of the FepA cork, TonB Q160C interacted with buried Cys substitutions within the FepA cork, the first such interactions seen with any TBDT. Both sets of interactions required active TonB. Taken together, these data suggest a model where the amphipathic helix binds to the TonB box, causing the mechanically weak domain of the FepA cork to dip sufficiently into the periplasmic space for interaction with the TonB Q160 region, which is an interaction that does not occur if the TonB box is deleted. The TonB amphipathic helix also interacted with periplasmic turns between FepA β-strands *in vivo* supporting a surveillance mechanism where TonB searched for TBDTs on the periplasmic face of the outer membrane.

bioRxiv preprint doi: https://doi.org/10.1101/2021.12.08.471779; this version posted December 8, 2021. The copyright holder for this preprint (which was not certified by peer review) is the author/funder. All rights reserved. No reuse allowed without permission.

# INTRODUCTION

The TonB system of *Escherichia coli* appears to be an answer to the challenges posed to Gram-negative bacteria by their dual membrane cell envelope. In particular, the outer membrane is a largely protective sieve with a diffusion cut-off of around 600 Da in *E. coli* (1). To capture large, scarce, essential nutrients, the outer membrane displays high-affinity customized β-barrels for active transport of diverse ligands (2). The energy for the active transport across the essentially unenergized outer membrane comes from a complex of cytoplasmic membrane proteins, TonB, ExbB, and ExbD. This complex harvests the cytoplasmic membrane proton gradient and transforms it into mechanical energy which drives vectoral transport of ligands through TBDTs and into the periplasmic space (3) (Fig. 1). Because these transporters bind directly only to TonB and not ExbB or ExbD during the energy transduction, they have been termed TonB-dependent transporters (TBDTs) (4). There is some confusion in the historical literature whereby they were first called TonB-dependent receptors because they were initially identified as receptors for colicins and bacteriophages, now known to be opportunistic agents (5-7). They have also been called TonB-gated transporters, TGTs, (8) and ligand-gated porins, LGPs, (9). *Escherichia coli* K12 encodes nine different TBDTs mostly devoted to acquisition of iron by various means with one devoted to cobalamin transport. While *E. coli* has dedicated TBDTs for a variety

bioRxiv preprint doi: https://doi.org/10.1101/2021.12.08.471779; this version posted December 8, 2021. The copyright holder for this preprint (which was not certified by peer review) is the author/funder. All rights reserved. No reuse allowed without permission.

of siderophores, enterochelin (a.k.a. enterobactin) is the single iron-chelating siderophore that *E. coli* synthesizes and excretes to capture iron from its environment [for a review see (10)]. The TBDT that provides for the recovery of iron-bearing enterochelin is FepA.

Each TBDT consists of a 22-stranded β-barrel, the lumen of which is occluded by an essential internal globular domain of ~ 150 residues called the cork (or hatch) [(11); for a review see (2)]. Because they are similar in structure, the results from one TBDT largely apply to most TBDTs. The mechanism by which TBDTs actively transport ligands such as the iron-siderophore enterochelin or cobalamin across the outer membrane remains a mystery, but there is general agreement that the cork must somehow move.

A TBDT cork has both a mechanically weak (approximately residues 1-70) and mechanically recalcitrant domain (approximately residues 70-150) both *in vivo* and *in vitro* (9, 12-14). An essential motif of five to seven mostly conserved residues known as the TonB box occupies the amino terminus of the mechanically weak domain. The TonB boxes of TBDTs are interchangeable, indicating that they do not mediate ligand specificity (15, 16).

The precise energy-transducing interaction of TonB with TBDTs has been challenging to define by structural determinations *in vitro* because ExbB and ExbD

bioRxiv preprint doi: https://doi.org/10.1101/2021.12.08.471779; this version posted December 8, 2021. The copyright holder for this preprint (which was not certified by peer review) is the author/funder. All rights reserved. No reuse allowed without permission.

functions, and the protonmotive force of the cytoplasmic membrane are all required for TonB-dependent energy transduction. Furthermore, *in vitro* and *in vivo* TonB binds to TBDTs regardless of its ability to transduce energy, (17-22), suggesting that certain residue-specific interactions result in energy transduction while other interactions fail to accomplish it.

The TonB protein is anchored in the cytoplasmic membrane by its hydrophobic amino terminal signal anchor with the rest of the protein (residues 33-239) occupying the periplasmic space [(23), Fig.1]. Interestingly, there are no essential residues in TonB (17, 24-28). In fact, even the His20 residue in the transmembrane domain can be replaced with non-protonatable Asn and retain full function, suggesting that the H20A mutation used in that study renders TonB inactive through steric distortion of its transmembrane domain in complex with ExbB and ExbD transmembrane domains (28).

There are, however, seven residues in the periplasmic TonB carboxy terminus (out of 90 sequentially scanned) that are functionally important (Y163, F180, G186, F202, W213, Y215, and F230) (27). With the exception of G186, these residues represent the complete set of aromatic residues in the last 90 residues of the carboxy terminus from 150-239, with the only other aromatic residue in the entire periplasmic domain (residues 33-239) being F125. We think these seven residues are the key because:

bioRxiv preprint doi: https://doi.org/10.1101/2021.12.08.471779; this version posted December 8, 2021. The copyright holder for this preprint (which was not certified by peer review) is the author/funder. All rights reserved. No reuse allowed without permission.

1) When substituted with Ala or Cys, each of these residues exhibits an idiosyncratic phenotype, with the profile of activities in four different assays being distinct for each of the seven substitutions (27, 29). They appear to be the means by which TonB discriminates among different TBDTs or possibly the colicins that parasitize them (30). In contrast, Cys substitution at the only other aromatic residue, TonB F125C, supports wild-type activity.

2) They are synergistic with one another such that any combination of two mutations (2 Ala, 2 Cys, or a combination) is completely inactive in all assays in a double mutant cycle analysis. For example, TonB F202A, W213A used in previous studies is completely inactive, whereas TonB F125A is not synergistic with substitutions at any of the seven residues (17, 27, 29). It therefore seems to set a maximal boundary on the active domain of the TonB carboxy terminus from G186 to F230, which contains a single amphipathic helix (residues 199-216).

3) Cys substitutions in five out of the seven important carboxy terminal residues (G186C, F202C, W213C, Y215C, F230C) are the only ones out of the 90 Cys substitutions that form disulfide-linked triplet homodimers (17, 27). While both inactive and active TonB binds to transporters, the disulfide-linked homodimers formed through the five Cys substitutions are trapped in configurations such that they no longer fractionate significantly with the outer membrane (17, 27). In contrast, TonB F125C, which appears to be outside the

bioRxiv preprint doi: https://doi.org/10.1101/2021.12.08.471779; this version posted December 8, 2021. The copyright holder for this preprint (which was not certified by peer review) is the author/funder. All rights reserved. No reuse allowed without permission.

149 active domain of the carboxy terminus, forms triplet homodimers that, like wild-
150 type TonB, still fractionate ~ 40% with the outer membrane, indicating that the
151 subsequent, more carboxy-terminal residues, including especially the amphipathic
152 helix, are free to undergo necessary conformational changes (31).

153 TonB is the limiting protein in the TonB system (32) and different TBDTs
154 must compete for its attention (33). TonB therefore interacts transiently with
155 ligand-loaded TBDTs in *E. coli* K12, giving rise to an energy transduction cycle
156 (67). Over the years we have defined stages in that cycle *in vivo*, the model for
157 which is depicted in Fig. 2.

158 In the model, the TonB carboxy termini of homodimers are conformationally
159 dynamic while the amino termini remain stably homodimerized throughout the
160 energy transduction cycle (31). Protonmotive force of the cytoplasmic membrane
161 is transduced into active transport at the outer membrane through sequential
162 contacts by the TonB carboxy terminus, first with itself, then with the ExbD
163 carboxy terminus, then with a TBDT (31). *In vivo* interaction sites between TonB
164 homodimers and between TonB-ExbD heterodimers have been identified, and a
165 common region between them is the TonB amphipathic helix (residues 199-216;
166 Fig. 3) (27, 34, 35). The primary goal of this study was to determine if the TonB
167 amphipathic helix played a role in contact with FepA.

bioRxiv preprint doi: https://doi.org/10.1101/2021.12.08.471779; this version posted December 8, 2021. The copyright holder for this preprint (which was not certified by peer review) is the author/funder. All rights reserved. No reuse allowed without permission.

Here we explored TonB interactions with three different regions of FepA—the TonB box, the cork, and the β-strand turns of the barrel. A novel *in vivo* interaction between Cys substitutions in the hydrophilic face of the essential TonB amphipathic helix and Cys substitutions in the essential FepA TonB box was identified. Interactions between TonB amphipathic helix and β-strand turns of the FepA barrel were identified, providing the first *in vivo* support for a surveillance model where TonB searches for a TBDT. The difference in interaction profiles with the mechanically weak domain of the FepA cork between the TonB amphipathic helix and TonB Q160 led to a model where the amphipathic helix pulls the mechanically weak domain of the FepA cork out of the barrel sufficiently that TonB Q160 interacts with otherwise buried residues.

bioRxiv preprint doi: https://doi.org/10.1101/2021.12.08.471779; this version posted December 8, 2021. The copyright holder for this preprint (which was not certified by peer review) is the author/funder. All rights reserved. No reuse allowed without permission.

## RESULTS

### *The carboxy terminal TonB amphipathic helix is essential for TonB system activity.*

The TonB region from ~ R158-N162, centered on TonB Q160 interacts with the TonB boxes of TBDTs *in vivo* [Fig. 4A; (4, 36)]. While the TonB box as a whole is essential for TBDT activity, its precise amino acid composition is tolerant of substitutions except for structure-breaking residues such as L8P in BtuB or I14P in FepA, substitutions that result in inactivation of the TBDT (4, 15, 36, 37). Even then, the TonB Q160 region still interacts with the BtuB L8P mutant TonB box *in vivo*, but in a different way (4).

Based on the position of residue Q160 within the TonB carboxy terminus, the solved crystal structures of TBDTs, and the solved crystal structures of TonB carboxy termini in complex with those TBDTs (Fig. 4B), it seems unlikely that Q160 contacts a TBDT without significant conformational changes to make the TonB box more accessible. The deletion of the proline rich domain that accounts for ~ 100 Å of TonB's reach to a TBDT has negligible effect upon its activity unless the periplasmic space is artificially expanded by transient exposure to high salt (24, 38, 39). This observation suggests that residues nearer the carboxy

bioRxiv preprint doi: https://doi.org/10.1101/2021.12.08.471779; this version posted December 8, 2021. The copyright holder for this preprint (which was not certified by peer review) is the author/funder. All rights reserved. No reuse allowed without permission.

terminus of TonB could be more important. There is also evidence that unknown regions in addition to the FepA TonB box and TonB Q160 are involved in transport (12, 40). Furthermore, the TonB Q160 region is not essential, suggesting that its role in contacting a TBDT is not essential (11).

The periplasmic TonB carboxy terminus contains an amphipathic helix (residues 199-216) which has been intriguing for many years (24, 29, 41). It includes three of the seven functional carboxy terminal residues, F202, W213 and Y215. To further explore the role the amphipathic helix plays in the mechanism of TonB-dependent energy transduction, we deleted the amphipathic helix codons 199-216 from plasmid pKP325, resulting in plasmid-encoded $TonB_{\Delta AH}$ (Fig. 5A). Plasmids expressing chromosomal levels of $TonB_{\Delta AH}$ (pKP476) were unable to complement KP1477 (Δ*tonB*) in cross-streaks against colicins B, Ia, and M, the most sensitive assays known for TonB function, requiring ~1 active TonB molecule per cell (42).

$TonB_{\Delta AH}$ fractionated on sucrose density gradients with ~ 60% located in the cytoplasmic membrane fractions and ~40% with the outer membrane fractions (Fig. 6A), the same proportions with which wild-type TonB fractionates (43). It is not known what causes TonB to bind sufficiently tightly to outer membrane components that ~ 40 % is pulled out of its complex with cytoplasmic membrane proteins ExbB and ExbD to fractionate with the outer membrane. One hypothesis

bioRxiv preprint doi: https://doi.org/10.1101/2021.12.08.471779; this version posted December 8, 2021. The copyright holder for this preprint (which was not certified by peer review) is the author/funder. All rights reserved. No reuse allowed without permission.

222 is that TonB outer membrane fractionation reflects a transient tight association
223 with outer membrane molecules--likely TBDTs--during Stage IV in the energy
224 transduction cycle (Fig. 2). While the region required for outer membrane
225 fractionation, residues 175-239, includes the amphipathic helix (43) and is
226 responsible for the ability of TonB to formaldehyde crosslink to FepA (37), this
227 result indicated that the amphipathic helix was not the region responsible for
228 fractionation of TonB with the outer membrane.

229 The inactivity of $TonB_{\Delta AH}$ could have been due to structural perturbation.
230 Alternatively, it could have been due to the simultaneous deletion of residues
231 F202, W213, and Y215, since combination of two Ala substitutions at any of those
232 residues renders TonB inactive (27, 29). Individual Cys substitutions from E203
233 through R212 have little phenotypic effect (27). To retain F202, W213, and Y215
234 and broadly restore the overall structure, we shifted the 10-amino acid core region
235 within the helix out of frame starting at residue 203 and shifted it back into frame
236 at residue 213 ($TonB_{fs}$, pKP372). The result for $TonB_{fs}$ was that the predicted
237 helical region was shortened slightly to encompass residues 201-209 (as analyzed
238 by JPRED), lost much of its amphipathic character, and at residue 210, Met was
239 substituted with Cys due to the frameshift (Fig. 5). Like $TonB_{\Delta AH}$, $TonB_{fs}$ was
240 completely insensitive in the colicin assays.

bioRxiv preprint doi: https://doi.org/10.1101/2021.12.08.471779; this version posted December 8, 2021. The copyright holder for this preprint (which was not certified by peer review) is the author/funder. All rights reserved. No reuse allowed without permission.

Due to the newly created M210C, $TonB_{fs}$ efficiently formed triplet homodimers. Like those of the Cys substitutions in functionally important residues, the $TonB_{fs}$ triplet homodimers fractionated essentially entirely with the cytoplasmic membrane, suggesting that they had trapped TonB at a stage in the energy transduction cycle before TonB associates with the outer membrane [Fig. 6B; (17, 27)]. TonB M210C in the context of otherwise wild-type residues is active and does not form triplet homodimers (27).

The *in vivo* dynamics of the TonB carboxy terminus suggest that it achieves a monomeric conformation at some point in the energy transduction cycle to allow productive interaction with FepA (31). Because a detectable proportion of $TonB_{fs}$ remained monomeric and was also found in the outer membrane on longer exposures (data not shown), its inactivity was not due to 100% entrapment as a triplet homodimer (Fig. 5B). We concluded that one or more aspects of the core amphipathic helix domain were required for TonB activity.

***The TonB amphipathic helix interacts functionally with the FepA TonB box.***

An analysis of whether and how the TonB amphipathic helix interacts *in vivo* with any of the TBDTs has never been performed. To investigate interactions between the TonB amphipathic helix and the FepA TonB box, we used *in vivo*

bioRxiv preprint doi: https://doi.org/10.1101/2021.12.08.471779; this version posted December 8, 2021. The copyright holder for this preprint (which was not certified by peer review) is the author/funder. All rights reserved. No reuse allowed without permission.

disulfide crosslinking of TonB and FepA Cys substitutions expressed at chromosomal levels, followed by electrophoresis on non-reducing SDS gels and immunoblotting with anti-TonB monoclonal antibodies.

We surveyed crosslinking by TonB amphipathic helix residues R204C, V206C, N208C, A209C, and R212C (Fig. 5). When expressed at chromosomal levels, each of the TonB Cys substitutions was at least 60% active in $^{55}$Fe-ferrichrome transport assays (Table 1). TonB Q160C, over 100% active and a known site of interaction with other TBDT TonB boxes, was also tested for comparison to the amphipathic helix Cys substitutions [Table 1; (4, 16)]. The FepA TonB box Cys substitutions tested were D12C, T13C, I14C, V15C, V16C and T17C; FepA T13C is fully active (44) as was FepA V16C (Table 1) with the rest assumed to be active.

The amphipathic helix substitutions at R204C, N208C and R212C formed disulfide-linked complexes with all FepA TonB box Cys residues except N208C with FepA T17C (for unknown reasons) (Fig. 7A). In contrast, TonB V206C and A209C did not form significant complexes with any of the FepA TonB box Cys residues, thus constituting a non-reactive hydrophobic face of the amphipathic helix. Steady state levels of monomeric TonB from samples in Fig. 7A are presented in Fig. 7B.

bioRxiv preprint doi: https://doi.org/10.1101/2021.12.08.471779; this version posted December 8, 2021. The copyright holder for this preprint (which was not certified by peer review) is the author/funder. All rights reserved. No reuse allowed without permission.

To determine if the TonB-FepA disulfide crosslinks were biologically relevant, each TonB Cys substitution was also paired with the H20A mutation in the TonB transmembrane domain (44). This mutation inhibits homodimerization of TonB through its carboxy terminus, a step necessary for formation of carboxy terminal TonB-ExbD heterodimers and the subsequent correct interaction of the TonB carboxy terminus with FepA [Figs. 2 and 4A, (18, 31)]. TonB H20A epitomizes the behavior of inactive TonB because it still interacts at unknown sites with FepA *in vivo* (17, 18). The TonB H20A mutation rendered all the TonB Cys substitutions inactive (Table 1).

The H20A mutation essentially eliminated complex formation by R204C, N208C and R212C, indicating that the H20 wild-type versions were engaging in biologically relevant interactions. The possibility that H20A somehow promoted new interactions with the hydrophobic face (substitutions V206C and A209C) was excluded since no complexes were observed. These results indicated that the TonB amphipathic helix contacted the essential FepA TonB box *in vivo*, consistent with its role in TBDT reception of TonB-transmitted energy. The TonB amphipathic helix is the first known alternative to the TonB Q160 region for contact with the FepA TonB box.

In the solved co-crystal structures of the TonB carboxy terminus with the TBDTs BtuB and FhuA, TonB residues R204, N208 and R212 of the amphipathic

bioRxiv preprint doi: https://doi.org/10.1101/2021.12.08.471779; this version posted December 8, 2021. The copyright holder for this preprint (which was not certified by peer review) is the author/funder. All rights reserved. No reuse allowed without permission.

300 helix interact with the barrels, but not the TonB boxes [Fig. 8, (20, 45)]. The lack
301 of interaction with the TonB amphipathic helix in those elegant co-crystal
302 structures supports the idea that the TonB carboxy terminus remains able to bind to
303 TBDTs and other proteins in an "un-energized" conformation (17, 18, 46, 47).
304
305 ***TonB Q160 interaction with the FepA TonB box is only partially dependent on***
306 ***TonB activity.***
307
308 Although the interaction of the TonB Q160 region with the TonB boxes of
309 several TBDTs has been well-documented both *in vivo* and *in vitro* (4, 15, 16, 48-
310 51), there has not yet been an analysis of how TonB Q160 interacts with the TonB
311 box of FepA nor an analysis of effects of inactive TonB upon any TBDT TonB box
312 interaction. In Fig. 7A, TonB Q160C crosslinked with all of the FepA TonB box
313 Cys substitutions, consistent with its behavior seen previously for BtuB Cys
314 substitutions in the TonB box (4). FepA V16C was chosen as the standard in all
315 subsequent experiments because it exhibited the highest degree of disulfide
316 crosslinking to TonB Q160C (Fig. 7A, left panel, lane 3), allowing comparisons of
317 relative levels of TonB-FepA complex formation.

bioRxiv preprint doi: https://doi.org/10.1101/2021.12.08.471779; this version posted December 8, 2021. The copyright holder for this preprint (which was not certified by peer review) is the author/funder. All rights reserved. No reuse allowed without permission.

318 The H20A mutation detectably decreased TonB Q160C crosslinking, but
319 without obliterating it altogether, suggesting that it represented a partially
320 functional interaction (Fig. 7A, left panel, compare lanes 3 and 4).

321 All of the interactions gave rise to an apparent higher and an apparent lower
322 mass complex within an approximate mass of one TonB plus one FepA (~ 116
323 kDa). [Although it has a calculated molecular mass of 26 kDa, TonB has an
324 apparent mass of 36 kDa on SDS gels because 17% of its residues are prolines
325 (41)]. Each of the two forms likely represented two different conformations made
326 by the same complex. First, because only a single unoxidized Cys exists in FepA
327 [because its two native Cys residues C487 and C494 are always oxidized (52)] and
328 in the TonB Cys substitutions studied here, all of which carry the C18G
329 substitution that removes the single native Cys. Second because the complexes are
330 also detected with anti-FepA polyclonal antibodies, ruling out participation of a
331 different protein (data not shown). And third, because similar doublets are also
332 seen with TonB-BtuB disulfide-linked complexes *in vivo* (4). That disulfide-linked
333 complexes can have different apparent masses depending on conformations of the
334 participants is exemplified by the three different disulfide-linked TonB
335 homodimers that result from a single TonB Cys substitution and demonstrably
336 occur on non-reducing SDS polyacrylamide gels (17).
337

bioRxiv preprint doi: https://doi.org/10.1101/2021.12.08.471779; this version posted December 8, 2021. The copyright holder for this preprint (which was not certified by peer review) is the author/funder. All rights reserved. No reuse allowed without permission.

338 ***Other FepA Cys substitutions assessed include the cork and periplasmic turns***
339 ***between β-strands of the barrel.***

340

341 Interaction of the TonB Cys substitutions with several additional FepA Cys
342 substitutions other than the TonB box was assayed to identify potential additional
343 sites of interaction by both the TonB amphipathic helix and Q160. In the
344 mechanically weak domain of the FepA cork, L23, S29, T32, A33, D34, and E35
345 are periplasmically accessible in the crystal structure. Residues A42, S46, and G54
346 are buried; T51 is partially buried. L85 is in the mechanically recalcitrant domain
347 and is partially buried [Fig. 9]. FepA residue T32, semi-conserved across TBDTs
348 (53), and the less-well-conserved A33 were included because they bind to TonB at
349 unknown sites and respond differentially to the presence and absence of ligand in
350 FepA photocrosslinking studies *in vivo* (40). G54 exhibits a modest change in
351 periplasmic exposure upon ligand binding (9).
352 FepA residues in the mechanically recalcitrant segment of the FepA cork
353 (V91, S92, S112, E120, V124, A131, V142, I145) were also evaluated to detect
354 possible cork movements not observed previously [(12) Fig. 10]. Also evaluated
355 were FepA R75, R126, E511, and E567, which form part of the "lock region", with
356 R75 and R126 in the recalcitrant domain of the FepA cork, and E511 and E567
357 positioned in the barrel (12, 14, 54). The lock region is proposed to be important

bioRxiv preprint doi: https://doi.org/10.1101/2021.12.08.471779; this version posted December 8, 2021. The copyright holder for this preprint (which was not certified by peer review) is the author/funder. All rights reserved. No reuse allowed without permission.

for transport but not binding of ligand, with the positively and negatively charged residues forming a structure that keeps the cork bound to the barrel [(36, 55, 56).

Contact with residues in periplasmic turns between β-strands of the FepA barrel, including the cork and barrel linker (D185, P243, D298, D356, D422, D455, D519, E576, D618, and D664; Fig. 11) were assessed, something that has not been investigated before for any TBDT. FepA residue E152, which marks the transition from cork to barrel and residue T722, the third residue from the carboxy terminus of FepA, were also included in the analysis.

Overall, 35 additional Cys substitutions in FepA were tested for their ability to form disulfide crosslinks with TonB Cys substitutions.

***TonB amphipathic helix interactions extend into the mechanically weak region of the FepA cork.***

To define the boundaries of reactive residues in the TonB amphipathic helix, the set of core TonB amphipathic helix Cys substitutions was expanded to include M201C and R214C (Fig. 5). Each TonB Cys substitution was assayed pairwise at least twice in combination with the 35 additional FepA Cys substitutions outside the TonB box.

bioRxiv preprint doi: https://doi.org/10.1101/2021.12.08.471779; this version posted December 8, 2021. The copyright holder for this preprint (which was not certified by peer review) is the author/funder. All rights reserved. No reuse allowed without permission.

Together, these results indicate that only Cys residues in the mechanically weak region of the FepA cork interacted with TonB Cys substitutions, whereas mechanically recalcitrant cork region (substitutions R75C through I145C) and the two lock region residues in the barrel, E511C and E567C were essentially non-reactive (Fig. 12A, B). Several interactions also occurred with FepA periplasmic β-strand turns (Fig. 12C). All interactions involved the same reactive face of the amphipathic helix that interacted with the TonB box: R204C, N208C, and R212C. TonB M201C and R214C gave little to no interaction with any FepA Cys, confirming the boundaries of the core reactive residues. A key observation for a model to be described in the discussion was that none of the core amphipathic helix Cys residues (R204C, N208C, and R212C) interacted detectably with FepA Cys substitutions that were buried in the crystal structure (A42C, S46C, T51C, and G54C) (Figs. 9, 12A).

TonB R204C made several H20-dependent contacts with most of the periplasmically-accessible FepA cork Cys residues (L23C, S29C, T32C, A33C, and D34C, but not E35C), with S29C and A33C interactions being the most abundant (Fig. 13A).

The only residue in the cork region significantly contacted by TonB N208C was FepA S29C and it was an H20-dependent interaction (Fig. 14A).

bioRxiv preprint doi: https://doi.org/10.1101/2021.12.08.471779; this version posted December 8, 2021. The copyright holder for this preprint (which was not certified by peer review) is the author/funder. All rights reserved. No reuse allowed without permission.

TonB R212C made the highest degree of H20-dependent contacts with FepA S29C—as high as the contacts between TonB Q160C and the FepA TonB box residue V16C, which were the highest we observed (Figs. 7, 14B).

FepA S29C appeared to be a hot spot since R204C, N208C, and R212C as well as the boundary-defining TonB M201C and R214C made complexes with it. FepA S29 is located close to the center of the first β-strand of the cork. It is within the region through which TonB could mechanically pull to unravel the cork as suggested before for FhuA (20), possibly as the site of *in vivo* TonB interaction at the as-yet-to-be-identified non-TonB box site prior to TonB box exposure (12).

***The TonB amphipathic helix interacts with periplasmic FepA β-strand barrel turns.***

*In vivo*, TonB interacts with FepA at one or more sites before it interacts with the FepA TonB box (12). Instead of FepA S29, the periplasmic β-strand turns of TBDTs could constitute such sites.

The last 150 residues of the TonB periplasmic domain, within which the amphipathic helix resides, have a calculated pI of 10.4 (41). It seemed logical that this TonB domain would be most likely to interact with the negatively charged residues of FepA barrel turns, where there appears to be one in nearly every turn

bioRxiv preprint doi: https://doi.org/10.1101/2021.12.08.471779; this version posted December 8, 2021. The copyright holder for this preprint (which was not certified by peer review) is the author/funder. All rights reserved. No reuse allowed without permission.

(except Pro243 in turn 2), including Glu152 in the linker region between cork and β-strand 1. Such interactions would likely be mediated through additional residues of TonB and FepA that would bring the now Cys-substituted residues into proximity (Fig. 11).

All of the FepA Cys substitutions in β-strand turns exhibited the ability to support fully wild-type levels of $^{55}$Fe-enterochelin transport except FepA E152C and T722C, where the levels dropped to ~ 60% (Table 1). Two Cys substitutions in the lock region of the barrel, E511C and E567C, were also assayed. FepA E511C had little effect on FepA activity, and E567C reduced activity to 65% of wild-type. Cys substitutions in the cork components of the lock region, R75C and R126C, reduced transport to ~40% of wild-type levels but did not eliminate it. Thus, neither the charged residues in the periplasmic β-strand turns nor the lock region residues were individually essential for FepA function.

Several sites of interaction between the TonB amphipathic helix residues R204C, N208C, and R212C and the periplasmic FepA β-strand barrel turns are summarized in Fig. 12C.

For TonB R204C, two different forms of the complex were observed, as was also seen with the FepA cork Cys substitutions (Fig. 13B). In contrast to interactions with the FepA cork, the apparent masses of the complexes with E152C, P243C, D298C, and D422C shifted to significantly higher values, highest

bioRxiv preprint doi: https://doi.org/10.1101/2021.12.08.471779; this version posted December 8, 2021. The copyright holder for this preprint (which was not certified by peer review) is the author/funder. All rights reserved. No reuse allowed without permission.

436 in the case of the latter three for unknown reasons. In contrast to interactions with
437 the cork, the β-strand barrel complexes were largely insensitive to the presence of
438 TonB H20A. Overall intensities of the complexes remained similar with both
439 TonB H20 and TonB H20A versions of R204C, but in the case of TonB H20A, the
440 complexes appeared to slightly shift their abundance to the higher mass complex—
441 again for unknown reasons.

442 For TonB N208C, weak interactions were detected with FepA E152C,
443 P243C, D298C, and D519C, each of which was H20-dependent (Fig. 14A). In
444 addition, TonB N208C made a very high level of contacts with D422C whether
445 TonB H20 or H20A was present. TonB R212C made a moderately high level of
446 H20-sensitive contacts with P243C, D422C, and D519C, whereas the contact with
447 D455C was largely H20-insensitive (Fig. 14B). Thus, both functional and non-
448 functional TonB amphipathic helix contacts occurred with the FepA β-strand turns.

449

450 ***TonB Q160 interactions include buried cork residues.***

451

452 Previous studies of TonB Q160C with TBDTs have been confined to the
453 TonB box. Since the TonB amphipathic helix made FepA contacts outside the
454 TonB box, we wanted to explore the possibility that Q160 did so as well.

bioRxiv preprint doi: https://doi.org/10.1101/2021.12.08.471779; this version posted December 8, 2021. The copyright holder for this preprint (which was not certified by peer review) is the author/funder. All rights reserved. No reuse allowed without permission.

455 Surprisingly, TonB Q160C interacted more widely than the amphipathic
456 helix did with Cys substitutions throughout the mechanistically weak part of the
457 FepA cork (Figs. 15A, B). Disulfide-linked heterodimers were observed between
458 TonB Q160C and FepA V16C, L23C, S29C, T32, A33C, D34C, E35C, A42C,
459 S46C and T51C, with the highest degree of interactions occurring with D34C and
460 S42C. The presence of the H20A mutation greatly diminished, and in most cases
461 eliminated, the crosslinking detected, suggesting that when TonB was inactive, the
462 ability of Q160C to make contacts within the mechanically weak domain of the
463 FepA cork was entirely prevented, unlike the interaction with the FepA TonB box
464 (Fig. 7A; 15C)

465 The disulfide crosslinking between TonB Q160C and FepA A42C or S46C
466 was notable because A42 and S46 are buried in the FepA crystal structure. TonB
467 Q160C crosslinks with FepA A42C were as abundant as those between the
468 standard TonB Q160C-FepAV16C pair (Figs. 9 and 15C). FepA A42 and S46 are
469 positioned in a plane approximately mid-way between top and bottom of the cork.
470 FepA A42 is on the interface with the FepA barrel. FepA S46 is entirely buried
471 within the cork (Fig. 9). These key observations are incorporated into a model in
472 the discussion.

473 TonB Q160C did not interact abundantly with any Cys substitutions more
474 carboxy-terminal than FepA T51C (Fig. 12). Consistent with cork movement,

bioRxiv preprint doi: https://doi.org/10.1101/2021.12.08.471779; this version posted December 8, 2021. The copyright holder for this preprint (which was not certified by peer review) is the author/funder. All rights reserved. No reuse allowed without permission.

475 weak H20-specific interactions with FepA G54C were also observed on long
476 exposures (Fig. 16, lane 5). Ma et al. previously observed modest periplasmic
477 exposure of FepA G54C in the presence of enterochelin (9). With the exception of
478 scarcely detectable interactions with D519C in a barrel turn, no interactions of
479 TonB Q160C with any of the remaining FepA Cys substitutions from V91C
480 through I145C (the mechanically recalcitrant domain), the lock region or the barrel
481 turns were detected no matter how long the exposures were (Figs. 12B and 12C;
482 data not shown). These observations form an important part of the model
483 presented in the discussion.
484
485 ***Deletion of the FepA TonB box prevents Q160C FepA cork interactions.***
486
487 Prior to the experiments above, the interaction of TonB Q160 with TBDT
488 sites other than their TonB boxes had not been tested. Since several additional
489 interactions were identified, we attempted to determine an order of events by
490 analyzing the effect of a FepA TonB box deletion on complex formation with the
491 FepA Cys substitution D34C with which TonB Q160C interacts with as abundantly
492 as it does the FepA TonB box, and G54C, which is buried and where the
493 interaction is weaker. In both cases, deletion of the FepA TonB box (residues 12-
494 17) essentially prevented the interaction (Fig. 16A, lanes 4 and 6). This finding

bioRxiv preprint doi: https://doi.org/10.1101/2021.12.08.471779; this version posted December 8, 2021. The copyright holder for this preprint (which was not certified by peer review) is the author/funder. All rights reserved. No reuse allowed without permission.

suggested that prior contact by unspecified TonB residues with the FepA TonB box was required for TonB Q160C to interact with FepA cork residues beyond the TonB box.

***TonB F202A, W213A lacks ExbD contact and inhibits the interaction of TonB Q160C with the FepA TonB box.***

In TonB, the F202A and W213A mutations boundary the core of the amphipathic helix and, in combination, completely inactivate it (29). TonB F202A, W213A was used as a tool to better understand parameters of the interaction between TonB Q160C and FepA V16C in the TonB box.

At the time when we discovered the inactivity of TonB F202A, W213A, the TonB-ExbD interaction captured by *in vivo* formaldehyde crosslinking of TonB had yet to be identified, however we knew that such double Ala mutations in the carboxy terminus did not prevent formation of the disulfide-linked TonB triplet homodimers (17, 29). In this study, the effect of the F202A, W213A mutation as well as another double Ala mutation--F202A, Y215A--was to prevent formation of the Stage III TonB-ExbD formaldehyde crosslinked heterodimer (18, 31). It was particularly telling that even when the TonB double Ala mutants were overexpressed, there was still no formation of the TonB-ExbD heterodimer, which

bioRxiv preprint doi: https://doi.org/10.1101/2021.12.08.471779; this version posted December 8, 2021. The copyright holder for this preprint (which was not certified by peer review) is the author/funder. All rights reserved. No reuse allowed without permission.

appears to play a key role in configuring TonB for successful energy transduction to FepA (Fig. 17; Fig. 2, Stage III TonB-ExbD heterodimers).

When F202 and W213 are mutated individually, they support intermediate and assay-specific levels of TonB activity (29). Consistent with that, the TonB Q160C, F202A substitution was still able to form the Q160C-V16C complex (Fig. lane 4). Although the presence of the F202A, W213A double mutations rendered TonB proteolytically unstable (Fig. 18, lane 5), as seen previously (29), it was possible to increase the exposure time of the immunoblot to the point where the level of monomer (Fig. 18, lane 6) was slightly greater than the level seen for the TonB Q160C and its F202A derivative (Fig. 18, lanes 3 and 4). In the longer exposure, it was clear that the ability of the TonB Q160C, F202A, W213A to form complexes with FepA V16C was significantly diverted away from the FepA TonB. Instead, the absence of a functional TonB carboxy terminus led Q160C to form three complexes, too small to be complexes with FepA. The location and spacing of the complexes were reminiscent of disulfide-linked TonB triplet homodimers that represent three different conformations of the TonB carboxy terminus *in vivo* (17).

## DISCUSSION

bioRxiv preprint doi: https://doi.org/10.1101/2021.12.08.471779; this version posted December 8, 2021. The copyright holder for this preprint (which was not certified by peer review) is the author/funder. All rights reserved. No reuse allowed without permission.

535 While TonB remains anchored in the cytoplasmic membrane by its amino
536 terminal transmembrane domain, the periplasmically localized TonB carboxy
537 terminus binds transiently and cyclically to TonB-dependent transporters (TBDTs)
538 in the outer membranes of Gram-negative bacteria to transduce cytoplasmic
539 membrane protonmotive force energy required for the active transport of ligands
540 (8). The *in vivo* molecular mechanism is not well understood. Previously, the only
541 known *in vivo* interaction between TonB and TBDTs involved the region of TonB
542 Q160 and the BtuB and FecA TonB boxes (4, 16, 50). Because our earlier studies
543 had suggested additional but unknown sites are involved *in vivo*, we searched for
544 site-specific interactions between TonB and FepA, the TBDT that transports the
545 sole siderophore synthesized and secreted by *E. coli* (12). TonB sites focused on
546 TonB Q160 and the TonB carboxy terminal amphipathic helix and their potential
547 interactions with sites in the FepA TonB box, in both mechanically weak and
548 mechanically recalcitrant domains of the FepA cork, and in FepA β-strand barrel
549 turns. It is important to study TonB interactions with TBDTs in their native
550 environment, where ExbB, ExbD and the protonmotive force of the cytoplasmic
551 membrane are all present (57).

552

553 ***The TonB carboxy terminal amphipathic helix is essential for the energy***
554 ***transduction cycle.***

bioRxiv preprint doi: https://doi.org/10.1101/2021.12.08.471779; this version posted December 8, 2021. The copyright holder for this preprint (which was not certified by peer review) is the author/funder. All rights reserved. No reuse allowed without permission.

555

556 TonB encoded from an amber mutation at codon 175 is inactive,
557 demonstrating that, although TonB Q160 has been the only site established to
558 interact with TBDTs, it is not sufficient for activity, and indicating that some
559 aspect of the last 65 TonB residues is essential (37). Within those last 65 residues,
560 we focused on the role of a sole amphipathic helix in the TonB carboxy terminus
561 (residues 199-216).

562 We found that the TonB amphipathic helix was essential either by deleting it
563 or by frameshifting it to maintain overall residue continuity. While this confirmed
564 the importance of the region, those results could also reflect an inability to form
565 TonB-TonB homodimers or TonB-ExbD heterodimers, both of which are
566 important for the energy transduction cycle (27, 31, 34, 35). We therefore asked if
567 the TonB amphipathic helix interacted directly with the only known essential
568 region of the TBDT, FepA, its TonB box.

569 Based on the *in vivo* disulfide crosslinking experiments, amphipathic helix
570 residues R204C, N208C and R212C defined a hydrophilic face that interacted with
571 Cys substitutions throughout the FepA TonB box, whereas the two residues on the
572 hydrophobic face, V206C and A209C did not interact with FepA. TonB R204C
573 was previously shown to be solvent exposed at some point in the energy
574 transduction cycle, consistent with localization on the hydrophilic face (58).

bioRxiv preprint doi: https://doi.org/10.1101/2021.12.08.471779; this version posted December 8, 2021. The copyright holder for this preprint (which was not certified by peer review) is the author/funder. All rights reserved. No reuse allowed without permission.

575 Because these *in vivo* interactions were prevented by the presence of the
576 inactivating TonB H20A mutation, they comprised a set of novel, functional, and
577 specific interactions that have been identified between TonB and a TBDT for the
578 first time.

579 The amphipathic helix interaction with the TonB box is absent from solved
580 co-crystal structures of the TonB carboxy terminus (~ residues 152-235) with
581 TBDTs BtuB and FhuA. The sidechains of the hydrophilic face residues R204C,
582 N208C, and R212C are oriented towards the TBDTs and distant from the TonB
583 boxes in both structures (20, 45), demonstrating either the difference between *in*
584 *vivo* "energized" and inactive TonB, or differences between TBDTs.

585 Now that an essential TonB component has been identified that interacts
586 with an essential FepA component (TonB box), it is tempting to speculate that the
587 TonB amphipathic helix holds the entire key to the TonB energy transduction cycle
588 for *E. coli.* As a result of this study and previous work, residues within the TonB
589 amphipathic helix have now been recognized to participate in sequential
590 interactions with three different proteins—TonB with itself, with ExbD and, here,
591 with FepA [(24, 59); Fig.2]. The amphipathic helix sequences are 55% conserved
592 (72% if E/D, R/K, and W/F substitutions are considered equivalent) amongst
593 enteric bacteria, but barely conserved with *Pseudomonas putida tonB*, which does
594 not complement an *E. coli tonB* mutation (24, 59).

bioRxiv preprint doi: https://doi.org/10.1101/2021.12.08.471779; this version posted December 8, 2021. The copyright holder for this preprint (which was not certified by peer review) is the author/funder. All rights reserved. No reuse allowed without permission.

595 Like wild-type TonB, TonB H20A formaldehyde-crosslinks with FepA *in*
596 *vivo*, but does not transmit energy to it (18, 28, 44). Formation of disulfide
597 crosslinks and their elimination by the inclusion of the TonB H20A mutation was a
598 clear indication that they represented functional interactions. While the lack of
599 disulfide-linked complexes for some pairs likely represented lack of interactions, it
600 could also be that the interactions could not be trapped due to due to misorientation
601 of the thiol side chains or because the interactions were too transient. It is also
602 likely that other important *in vivo* regions of interactions remain to be discovered.
603
604 ***A model: does the FepA cork "fish" for the TonB Q160 region?***
605
606 On the face of it, the amphipathic helix region (residues 199-216) of TonB is
607 more logical than TonB Q160 as a site of initial contact with a TBDT TonB box
608 because it is theoretically somewhat closer to the outer membrane. This is
609 especially so since ~ 100 Å of TonB's reach across the periplasmic space is due to
610 the proline-rich domain (residues 70-102), which can be deleted without
611 eliminating TonB activity [Fig. 4; (24, 39)]. In addition, the amphipathic helix is
612 essential, whereas TonB Q160 and the region encompassing it (residues R158-
613 Q162) can be deleted without inactivating TonB (26). Why this region has been a

bioRxiv preprint doi: https://doi.org/10.1101/2021.12.08.471779; this version posted December 8, 2021. The copyright holder for this preprint (which was not certified by peer review) is the author/funder. All rights reserved. No reuse allowed without permission.

source of second site suppressors for inactive TBDT TonB box mutations remains a mystery (48, 49).

Because it is not essential, the wide range of *in vivo* contacts made by TonB Q160C was surprising, encompassing not only the FepA TonB box seen previously for other *E. coli* TBDTs but also, for the first time, residues throughout the region of the mechanically weak domain of the FepA cork. Most importantly, two of the interacting residues (A42, and S46) are buried within in the FepA cork (60). In contrast to the partially H20-senstive Q160C interactions with the FepA TonB box, both of these contacts were completely prevented if the TonB Q160C also carried the inactivating H20A mutation, indicating that they fully represented the action of functional TonB. The FepA region of TonB Q160C interaction ended just prior to the beginning of the mechanically recalcitrant domain of the FepA cork.

TonB Q160C interacted as abundantly with FepA A42C as it did with the FepA V16C standard within the TonB box, which was the most abundant interaction seen in this entire study. Because FepA A42C is buried, this strongly suggested that enough of the cork domain entered the periplasm to expose A42C, along with S46C, to interaction with TonB Q160C. Our previous discovery of 20-to-25-fold increases in periplasmic accessibility of the buried cork residues A42C, S46C (and the partially buried T51C) in response to the addition of colicin B ligand *in vivo* validates the finding here that at some point in the energy

bioRxiv preprint doi: https://doi.org/10.1101/2021.12.08.471779; this version posted December 8, 2021. The copyright holder for this preprint (which was not certified by peer review) is the author/funder. All rights reserved. No reuse allowed without permission.

transduction cycle, these residues become available for interaction with TonB Q160C and likely neighboring residues (4, 12). In striking contrast, none of the amphipathic helix Cys substitutions interacted with FepA Cys substitutions that were buried within the cork, with targets limited to periplasmically accessible Cys residues.

The overall non-reactivity of the mechanically recalcitrant domain of FepA in this *in vivo* study also validated our earlier finding of its resistance to being periplasmically labeled in the presence of a large (~55 kDa) ligand, colicin B. In that study, two distinct possibilities were proposed for the mechanically recalcitrant domain: first that it did not move and second that it moved but was blocked from being labeled by the presence of another protein (12). Our studies here did not exclude either possibility. For the first possibility to be true, colicin B would need to denature on its way through a small opening, which, given its size and structure as a dumbbell that fills the FepA lumen, seems unlikely (61). Nonetheless, such denaturation has been observed for the amino-terminal domain of colicin pyoS2 of *P. aeruginosa* through its TBDT FpvA *in vivo* (62). Furthermore, the significantly smaller (~29 kDa) colicin M, which parasitizes the TBDT FhuA, uses a chaperone to fold it in the periplasm where it inhibits peptidoglycan formation (63). A mechanically recalcitrant domain for the TBDT BtuB has been characterized *in vitro* (14).

bioRxiv preprint doi: https://doi.org/10.1101/2021.12.08.471779; this version posted December 8, 2021. The copyright holder for this preprint (which was not certified by peer review) is the author/funder. All rights reserved. No reuse allowed without permission.

While it is not possible to definitively turn static data into a dynamic model, these results suggested a possible sequence of events where the TonB amphipathic helix binds to the FepA TonB box, which moves the FepA cork sufficiently that its mechanically weak domain extends into the periplasm. Previously buried cork residues are thus able to "fish" for interactions with various sites on TonB, among which we captured the TonBQ160C interaction. It is notable that the hydrophilic face of the amphipathic helix contacted multiple residues in the β-strand turns of the FepA barrel, whereas TonBQ160C could contact none of them, consistent with the idea that it does not reach that far across the periplasmic space. These results may also explain why the Q160 region of TonB is not essential—it is secondary and incidental to the action of the TonB amphipathic helix at the FepA TonB box.

Consistent with this model, without the FepA TonB box present for the amphipathic helix to engage, TonB Q160C did not interact at either a residue central to the mechanically weak FepA domain (D34C) or a residue at its near boundary with the mechanically recalcitrant FepA domain (G54C).

The combination of F202A, W213A mutations on either side of the TonB amphipathic helix substantially inhibited the normal interaction of TonB Q160C with FepA TonB box residue V16C. As such, the double TonB mutation somewhat mimicked the effect of the FepA TonB box deletion that prevented Q160C interactions with FepA D34C and G54C, suggesting that TonB F202A,

bioRxiv preprint doi: https://doi.org/10.1101/2021.12.08.471779; this version posted December 8, 2021. The copyright holder for this preprint (which was not certified by peer review) is the author/funder. All rights reserved. No reuse allowed without permission.

674 W213A might have inhibited the amphipathic helix from engaging the FepA TonB
675 box, preventing the FepA cork from fishing for TonB Q160C.

676 Consistent with our results revealing movement of the FepA cork, Majumdar
677 et al. engineered intra-cork disulfide bonds in FepA, most of which significantly
678 decreased Fe-enterochelin transport. The transport was restored in the presence of
679 reducing agent, indicating that there are required conformational changes within
680 the cork itself (52).

681

682 ***Comparison to results from* in vivo *photocrosslinking to study FepA dynamics***

683

684 We previously identified FepA residues that interact with TonB using *in vivo*
685 photocrosslinking by the reagent pBpa inserted at sites of engineered amber
686 substitutions in *fepA* (40). A potential conformational switch signaling to TonB
687 that ligand (enterochelin) is bound was identified. FepA T32pBpa bound TonB in
688 the absence enterochelin whereas FepA A33pBpa bound TonB in its presence. In
689 the current study, both FepA T32C and A33C interactions occurred with both
690 TonB R204C in the amphipathic helix and Q160C without discrimination, perhaps
691 reflecting an average of ligand-bound and unbound states for FepA. FepA
692 S29pBpa, A42CpBpa, S46pBpa, and T51pBpa in the mechanically weak domain
693 did not significantly photocrosslink to TonB, even though these variants all

bioRxiv preprint doi: https://doi.org/10.1101/2021.12.08.471779; this version posted December 8, 2021. The copyright holder for this preprint (which was not certified by peer review) is the author/funder. All rights reserved. No reuse allowed without permission.

694 supported ~ 75% activity. This could be because the interactions are too rapid to
695 capture, whereas in the current study, the disulfide bond formations would
696 potentially have been aided by the DsbA system (64).

697 Although the effect of a *dsbA* mutation on disulfide formation in this study
698 was not tested, the effect on TonB triplet homodimer formation are informative
699 and suggest that the frustrating answer is: it depends. Plasmids expressing TonB
700 F125C, G186C, F202C, W213C, Y215C, or F230C substitutions were transformed
701 into an isogenic *dsbA* strain, KP1514 [W3110, Δ(*tonB, P14*::*blaM)*, *dsbA*::*kan*],
702 and the degree of disulfide-linked triplet homodimer formation was compared to
703 previous results from a *dsbA*+ strain (27). TonB F125C, TonB Y215C and TonB
704 F230C showed greatly diminished triplet dimer formation in the absence of DsbA,
705 with an intermediate decrease for W213C. In no case was triplet dimer formation
706 entirely abolished. For TonB F202C and TonB G186C, there was no effect of the
707 *dsbA* mutation (Spicer and Postle, unpublished data).

708 In contrast to the present study, FepA E120pBpa and I145pBpa on the
709 periplasmic face of the FepA cork, did photocrosslink to TonB (40). We do not
710 have an explanation for these differences but note that the techniques are
711 dissimilar, and the disulfide crosslinking studies here were congruent with our
712 studies of *in vivo* FepA cork accessibility (12).

713

bioRxiv preprint doi: https://doi.org/10.1101/2021.12.08.471779; this version posted December 8, 2021. The copyright holder for this preprint (which was not certified by peer review) is the author/funder. All rights reserved. No reuse allowed without permission.

714 ***Current* in vivo *approaches are not amenable to discovery of TonB aromatic***
715 ***residue contacts with FepA.***

716

717 This study revealed the importance of the TonB amphipathic helix core
718 (residues 204-212) in contacting the TonB box of FepA. However, individual Cys
719 substitutions within that core have no phenotype (27). Similarly, the sequences of
720 TBDT TonB boxes contain little residue-specific information and indeed can be
721 swapped for one another (15, 16). It is therefore unlikely that this set of
722 interactions is responsible for the idiosyncratic phenotypes observed for Cys and
723 Ala substitutions of the aromatic residues that boundary the amphipathic helix
724 core—F202 and W213 among others.

725 We have been, unfortunately, thwarted in our ability to define the sites on
726 FepA where TonB F202 and W213 interact due to two factors, both based on
727 signal-to-noise ratios. First, Cys substitutions at these aromatic residues form a
728 sufficiently high abundance of disulfide-linked triplet homodimers *in vivo* that any
729 side reactions would be swamped out and difficult to interpret (17, 27). Second,
730 there appears to be a region of TonB that cannot be analyzed by in vivo
731 photocrosslinking. We previously used targeted amber mutations in *fepA* and in
732 *exbD* to guide insertion of the photocrosslinkable amino acid pBpa and generate
733 crosslinks at unknown sites in TonB *in vivo*. In those studies, both the *fepA* and

bioRxiv preprint doi: https://doi.org/10.1101/2021.12.08.471779; this version posted December 8, 2021. The copyright holder for this preprint (which was not certified by peer review) is the author/funder. All rights reserved. No reuse allowed without permission.

734 *exbD* amber mutations fully incorporate the pBpa and result in full-length proteins
735 (40, 65).

736 We were hopeful that a reciprocal approach using targeted amber mutations
737 in *tonB* at the carboxy terminal aromatic residues would be fruitful, however, we
738 were thwarted by failure to incorporate sufficient pBpa, except small amounts and
739 only after highest overexpression, such that ~ 85-100% of the TonB was present as
740 the truncated amber mutant form or its degradation product. Given the dominant
741 negative gene dosage effect of *tonB* overexpression, the high level of incomplete
742 TonB fragments would have obscured meaningful interpretations (3, 66). There
743 may be something unusual about this particular region of *tonB* during translation
744 since we have been able to successfully incorporate pBpa into *tonB* at engineered
745 amber sites in the transmembrane domain (Postle and Guzek, unpublished data).

746

747 ***Surveillance of FepA periplasmic β-strand turns***

748

749 TonB binds to transporters whether or not it is "energized", although it is
750 still not clear what that term means mechanistically. For example, inactive TonB
751 H20A formaldehyde-crosslinks to FepA *in vivo* (18) and purified inactive carboxy
752 terminal domains of TonB bind with varying affinities to purified transporters *in*
753 *vitro* (19, 21, 22). Here we identified the first *in vivo* interactions between the

bioRxiv preprint doi: https://doi.org/10.1101/2021.12.08.471779; this version posted December 8, 2021. The copyright holder for this preprint (which was not certified by peer review) is the author/funder. All rights reserved. No reuse allowed without permission.

754 TonB amphipathic helix and the FepA β-strand turns, the majority of which
755 appeared to represent interactions with inactive TonB.

756 The periplasmic β-strand turns are candidates for one or more TonB-FepA
757 binding sites since they protrude more deeply into the periplasm than the face of
758 the cork does (Fig. 11). We chose Cys substitutions at Asp or Glu residues (and
759 Pro243) in the periplasmic β-strand turns as most likely to be required for FepA
760 activity and were surprised they were all functional. The fact that they had little to
761 no effect on activity, builds on and confirms a tolerance to mutation that generally
762 characterizes TBDTs (36, 40), where only certain structurally disruptive mutations
763 such as a Leu-to-Pro mutation in the TonB box, its complete deletion, or Arg-to-
764 Pro in the lock region residue 75 lead to TBDT inactivation (4, 15, 55).

765 Interaction of TonB N208C with the FepA periplasmic β-strand turn 5
766 D422C variant was striking for two reasons: first, because it was so abundant--as
767 abundant as the control TonB Q160C-FepA V16C interaction, and second because
768 it was impervious to the presence of the inactivating TonB H20A substitution. In
769 contrast, TonB R212C formed complexes with Cys residues in several β-strand
770 turns, the majority of which decreased if TonB was inactivated by the H20A
771 mutation.

772 Phage panning using a purified TonB carboxy terminus identifies TonB
773 interaction sites on FhuA sites corresponding to barrel turns 1 and 2, represented in

bioRxiv preprint doi: https://doi.org/10.1101/2021.12.08.471779; this version posted December 8, 2021. The copyright holder for this preprint (which was not certified by peer review) is the author/funder. All rights reserved. No reuse allowed without permission.

774 this study by FepA D185C and P243C (56). We did not observe interaction of
775 TonB with D185, but we did observe R204C, N208C and R212C interacting with
776 P243C; interactions by N208C and R212C were both H20-dependent.

777 Considering all the results, this study demonstrated that the hydrophilic face
778 of the essential TonB amphipathic helix was used for contacts throughout FepA. It
779 also validated the idea that, *in vivo*, there are certain TonB-FepA contacts made by
780 active TonB, with a different set of contacts that do not lead to energy transduction
781 events. The contacts made by inactive "unenergized" TonB, some of which were
782 quite abundant, could be consistent with membrane surveillance and
783 conformational sampling (27, 46) where TonB discriminates between a TBDT and
784 a porin, or searches for a ligand-loaded TBDT (67). Because the ligand
785 enterochelin was present throughout the experiments here, it will be important to
786 determine which TonB-FepA interaction sites are ligand-dependent. If any *in vivo*
787 TonB-FepA interactions are H20-dependent as well as ligand-dependent, they
788 would constitute candidates important for energy transduction.

789

790

bioRxiv preprint doi: https://doi.org/10.1101/2021.12.08.471779; this version posted December 8, 2021. The copyright holder for this preprint (which was not certified by peer review) is the author/funder. All rights reserved. No reuse allowed without permission.

# METHODS AND MATERIALS

## *Bacterial strains & plasmids*

The strains and plasmids used in this study are listed in Table 2. All bacteria are derivatives of *Escherichia coli* K-12 strain W3110. KP1491 was constructed by $P1_{vir}$ transduction of the Δ(*tonB, P14)::blaM* cassette from KP1477 into KP1489 (W3110 Δ*fepA*).

Plasmids pKP1858 and pKP1859 were created from pKP476 and pKP372 respectively, using polymerase chain reaction (PCR)-based site-directed mutagenesis as previously described (26) to create C18G substitutions in both plasmids. The majority of plasmids encoding *tonB* mutants were derived from pKP1362 (*tonB* C18G), which was constructed by cloning *tonB* C18G from pKP568 into the Sph1 site of pPro33, allowing for expression from the propionate promoter (68). Plasmids encoding *fepA* mutants were derived from pKP515 where *fepA* is expressed from the arabinose promoter in pBAD24 (11). Mutations were engineered through PCR-based site-directed mutagenesis as previously described (26). The coding region of each engineered mutant gene was confirmed through Sanger sequencing at the Pennsylvania State University Nucleic Acid Facility.

## *Growth media and culture conditions*

bioRxiv preprint doi: https://doi.org/10.1101/2021.12.08.471779; this version posted December 8, 2021. The copyright holder for this preprint (which was not certified by peer review) is the author/funder. All rights reserved. No reuse allowed without permission.

Liquid cultures were grown at 37°C with aeration in LB broth or in M9 minimal salts supplemented with 1% glycerol, 0.2% vitamin-free casamino acids, 40 μg $ml^{-1}$ of tryptophan, 4 μg $ml^{-1}$ of thiamine, 1 mM $MgSO_4$ and 0.5 mM $CaCl_2$. For disulfide-crosslinking, the M9 minimal salts medium was further supplemented with 10 μM Fe (as ferric chloride). For [$^{55}$Fe]-enterochelin transport assays, the M9 minimal salts medium was supplemented with 1.85 μM Fe (as ferric chloride) as well as 40 μg $ml^{-1}$ of tyrosine and 40 μg $ml^{-1}$ of phenylalanine to facilitate growth of *aroB* strains on which they were performed (69). Chloramphenicol at 34 μg $ml^{-1}$ and ampicillin at 100 μg $ml^{-1}$ were used to maintain TonB and FepA plasmids respectively. The TonB plasmids were induced with the following concentrations with sodium propionate to achieve chromosomal levels; TonB C18G (10 mM), TonB C18G M201C (10 mM), TonB C18G R204C (0.5 mM), TonB C18G V206C (10 mM), TonB C18G N208C (10 mM), TonB C18G A209C (10 mM), TonB C18G R212C (1 mM), TonB C18G R214C (10 mM), all TonB C18G H20A cysteine substitutions (15 mM). FepA cysteine substitutions were not induced as the base expression level approximated chromosomally encoded FepA levels in cells grown with 1.85 μM Fe.

***Sucrose density gradient fractionations***

bioRxiv preprint doi: https://doi.org/10.1101/2021.12.08.471779; this version posted December 8, 2021. The copyright holder for this preprint (which was not certified by peer review) is the author/funder. All rights reserved. No reuse allowed without permission.

Sucrose density gradient fractionation was carried out essentially as described previously (43) with some modifications. Strain KP1344 containing plasmids pKP1858 or pKP1859 was grown as described above, in the presence of 0.002% arabinose and 0.1% arabinose respectively, to mid exponential phase. Cells were harvested and lysed by French pressure cell at 4° C. The cell lysate supernatant was applied to the top of the sucrose gradient and centrifuged in a Beckman SW40 rotor at 35,000 r.p.m. for 19 hours at 4° C. Collected fractions were precipitated with an equivalent volume of 20% trichloroacetic acid (TCA) at 4° C, and suspended in Laemmli sample buffer (70) (LSB) at 95ºC for 5 minutes. 10 µl of each sample was electrophoresed on 12% SDS-polyacrylamide gels and then immunoblotted with TonB 4F1 monoclonal antibodies (71).

**In vivo *formaldehyde crosslinking***

Strains were subcultured 1:100 from saturated LB cultures into supplemented M9 minimal salts medium supplemented with L-arabinose as described in the Figure 17 legend and 34 µg $ml^{-1}$ chloramphenicol without added iron. Cells were harvested at an $A_{550}$ of 0.5 in 1 ml aliquots, centrifuged and aspirated. The pellet was suspended in 938 µl of 100 mM sodium phosphate buffer at pH 6.8 to which 62.5 µl of 16% formaldehyde was added and incubated for 15 minutes at 22ºC. Cells were then pelleted, suspended in 50 µl of 2x LSB (twice the

bioRxiv preprint doi: https://doi.org/10.1101/2021.12.08.471779; this version posted December 8, 2021. The copyright holder for this preprint (which was not certified by peer review) is the author/funder. All rights reserved. No reuse allowed without permission.

usual concentration) and heated for 5 minutes at 60ºC. The samples were electrophoresed on 11% SDS-polyacrylamide gels and then immunoblotted with TonB 4F1 monoclonal antibodies or anti-ExbD polyclonal antibodies (32, 71).

**In vivo *disulfide crosslinking***

KP1491 harboring pairwise combinations of plasmid-encoded TonB and plasmid encoded FepA were subcultured 1:100 from saturated LB cultures into supplemented M9 minimal salts medium and grown with appropriate antibiotics to $A_{550}$ = 0.45. 0.4 OD $ml^{-1}$ of cells were harvested by centrifugation and precipitated with an equal volume of 4ºC 20% TCA to stop the proteolysis of TonB that occurs in LSB at 95°C when TCA is not used (72). The TCA-precipitated pellets were boiled at 95ºC for 10 minutes in 100 µl of LSB with 50 mM iodoacetamide to block any remaining free cysteines to prevent *in vitro* disulfide crosslinking. All samples were analyzed on 9% SDS-PAGE gels and followed by immunoblot analysis with TonB 4F1 monoclonal antibody and FepA polyclonal antibodies (32).

To eliminate the possibility that disulfide crosslinks formed due to the presence of TCA during cell harvesting, the efficiency of crosslinking was compared with and without TCA precipitation. Upon harvesting cells were pelleted without TCA. The cell pellets were boiled at 95ºC for 10 minutes in 100

bioRxiv preprint doi: https://doi.org/10.1101/2021.12.08.471779; this version posted December 8, 2021. The copyright holder for this preprint (which was not certified by peer review) is the author/funder. All rights reserved. No reuse allowed without permission.

µl of LSB with 50 mM iodoacetamide. TCA slightly enhanced the recovery of both crosslinked complexes, which also still formed in the absence of TCA and the monomer such that levels of crosslinking were proportional to the controls with and without TCA (data not shown).

### [$^{55}$*Fe*]-*enterochelin transport*

TonB and FepA with individual Cys substitutions were assessed for their initial rates of enterochelin (Sigma-Aldrich) transport as described previously (40). FepA constructs were assayed in KP1490 (W3110 *aroB* Δ*fepA*) whereas TonB constructs were assayed in strain KP1406 (W3110 *aroB* Δ(*tonB, P14)::blaM*). Enterochelin is the sole siderophore synthesized and secreted by *E. coli* K12. The *aroB* mutation prevents enterochelin synthesis and the synthesis of any intermediates that could interfere in the assay (69).

## ACKNOWLEDGEMENTS

We thank Ryan Guzek for analysis of the TonB pBpa substitutions and construction of pKP1836 and pKP1837; Bradley Spicer for construction of pKP1382, pKP1400, pKP1403, pKP1427, FepA Cys substitutions in the TonB

bioRxiv preprint doi: https://doi.org/10.1101/2021.12.08.471779; this version posted December 8, 2021. The copyright holder for this preprint (which was not certified by peer review) is the author/funder. All rights reserved. No reuse allowed without permission.

box, and analyzing effects of a *dsbA* strain on TonB triplet homodimer formation; Suzanne Wardell for construction of pKP372; Shaima El Mowafi for construction of pKP1369 and pKP1370; Siti Kamarudin for construction of pKP1858, pKP1859, and pKP1861; Surendran Devanathan for construction of KP1491; Cheryl Swayne for construction of pKP1362; Raka Ghosh for construction of pKP1581; Yu-An Liu for construction of pKP1361; Larissa Goldman for construction of pKP1506; Gui Teng Chua for construction of pKP1841, pKP1850, and pKP1854; Elizabeth McFadden for the formaldehyde crosslinking experiment on the TonB double Ala variants, and Glenn Hwang for construction of pKP2299, pKP2303, pKP2304, the analysis of amphipathic helix Cys substitutions interactions with the FepA TonB box and excellent technical assistance. We thank the *E. coli* Genetic Stock Center and the Jonathan Beckwith lab for their *dsbA*::kan strain, RI90. Support from NIGMS grant GM112710 is gratefully acknowledged.

bioRxiv preprint doi: https://doi.org/10.1101/2021.12.08.471779; this version posted December 8, 2021. The copyright holder for this preprint (which was not certified by peer review) is the author/funder. All rights reserved. No reuse allowed without permission.

# REFERENCES

1. **Nikaido H.** 2003. Molecular basis of bacterial outer membrane permeability revisited. Microbiol Mol Biol Rev **67:**593-656.

2. **Noinaj N, Guillier M, Barnard TJ, Buchanan SK.** 2010. TonB-dependent transporters: regulation, structure, and function. Annu Rev Microbiol **64:**43-60.

3. **Fischer E, Günter K, Braun V.** 1989. Involvement of ExbB and TonB in transport across the outer membrane of *Escherichia coli*: phenotypic complementation of *exb* mutants by overexpressed *tonB* and physical stabilization of TonB by ExbB. J. Bacteriol. **171:**5127-5134.

4. **Cadieux N, Kadner RJ.** 1999. Site-directed disulfide bonding reveals an interaction site between energy-coupling protein TonB and BtuB, the outer membrane cobalamin transporter. Proc. Natl. Acad. Sci. USA **96:**10673-10678.

5. **Davies JK, Reeves P.** 1975. Genetics of resistance to colicins in *Escherichia coli* K-12: cross-resistance among colicins of group B. J. Bacteriol. **123:**96-101.

6. **Pugsley AP, Reeves P.** 1976. Increased production of the outer membrane receptors for colicins B, D and M by *Escherichia coli* under iron starvation. Biochem. Biophys. Res. Commun. **70:**846-853.

bioRxiv preprint doi: https://doi.org/10.1101/2021.12.08.471779; this version posted December 8, 2021. The copyright holder for this preprint (which was not certified by peer review) is the author/funder. All rights reserved. No reuse allowed without permission.

923 7. **Frost GE, Rosenberg H.** 1975. Relationship between the *tonB* locus and
924 iron transport in *Escherichia coli*. J. Bacteriol **124:**704-712.
925 8. **Gresock MG, Savenkova MI, Larsen RA, Ollis AA, Postle K.** 2011.
926 Death of the TonB shuttle hypothesis. Front. Microbiol. **2:**206.
927 9. **Ma L, Kaserer W, Annamalai R, Scott DC, Jin B, Jiang X, Xiao Q,**
928 **Maymani H, Massis LM, Ferreira LC, Newton SM, Klebba PE.** 2007.
929 Evidence of ball-and-chain transport of ferric enterobactin through FepA. J. Biol.
930 Chem. **282:**397-406.
931 10. **Klebba PE, Newton SMC, Six DA, Kumar A, Yang T, Nairn BL,**
932 **Munger C, Chakravorty S.** 2021. Iron acquisition systems of Gram-negative
933 bacterial pathogens define TonB-dependent pathways to novel antibiotics. Chem.
934 Rev. **121:**5193-5239.
935 11. **Vakharia HL, Postle K.** 2002. FepA with globular domain deletions lacks
936 activity. J. Bacteriol. **184:**5508-5512.
937 12. **Devanathan S, Postle K.** 2007. Studies on colicin B translocation: FepA is
938 gated by TonB. Mol. Microbiol. **65:**441-453.
939 13. **Udho E, Jakes KS, Finkelstein A.** 2012. TonB-dependent transporter FhuA
940 in planar lipid bilayers: partial exit of its plug from the barrel. Biochemistry
941 **51:**6753-6759.

bioRxiv preprint doi: https://doi.org/10.1101/2021.12.08.471779; this version posted December 8, 2021. The copyright holder for this preprint (which was not certified by peer review) is the author/funder. All rights reserved. No reuse allowed without permission.

14. **Hickman SJ, Cooper REM, Bellucci L, Paci E, Brockwell DJ.** 2017. Gating of TonB-dependent transporters by substrate-specific forced remodelling. Nat. Commun. **8:**14804.

15. **Gudmundsdottir A, Bell PE, Lundrigan MD, Bradbeer C, Kadner RJ.** 1989. Point mutations in a conserved region (TonB Box) of the *Escherichia coli* outer membrane BtuB protein affect vitamin B12 transport. J. Bacteriol. **171:**6526-6533.

16. **Ogierman M, Braun V.** 2003. Interactions between the outer membrane ferric citrate transporter FecA and TonB: studies of the FecA TonB box. J. Bacteriol. **185:**1870-1885.

17. **Ghosh J, Postle K.** 2005. Disulphide trapping of an *in vivo* energy-dependent conformation of *Escherichia coli* TonB protein. Mol. Microbiol. **55:**276-288.

18. **Ollis AA, Manning M, Held KG, Postle K.** 2009. Cytoplasmic membrane protonmotive force energizes periplasmic interactions between ExbD and TonB. Mol. Microbiol. **73:**466-481.

19. **Koedding J, Howard SP, Kaufman L, Polzer P, Lustig A, Welte W.** 2004. Dimerization of TonB is not essential for its binding to the outer membrane siderophore receptor FhuA of *E. coli.* J. Biol. Chem. **279:**9978-9986.

bioRxiv preprint doi: https://doi.org/10.1101/2021.12.08.471779; this version posted December 8, 2021. The copyright holder for this preprint (which was not certified by peer review) is the author/funder. All rights reserved. No reuse allowed without permission.

20. **Pawelek PD, Croteau N, Ng-Thow-Hing C, Khursigara CM, Moiseeva N, Allaire M, Coulton JW.** 2006. Structure of TonB in complex with FhuA, *E. coli* outer membrane receptor. Science **312:**1399-1402.

21. **Khursigara CM, De Crescenzo G, Pawelek PD, Coulton JW.** 2004. Enhanced binding of TonB to a ligand-loaded outer membrane receptor. Role of the oligomeric state of TonB in formation of a functional FhuA-TonB complex. J. Biol. Chem. **279:**7405-7412.

22. **Freed DM, Lukasik SM, Sikora A, Mokdad A, Cafiso DS.** 2013. Monomeric TonB and the Ton Box are required for the formation of a high-affinity transporter-TonB complex. Biochemistry **52:**2638-2648.

23. **Postle K, Skare JT.** 1988. *Escherichia coli* TonB protein is exported from the cytoplasm without proteolytic cleavage of its amino terminus. J. Biol. Chem. **263:**11000-11007.

24. **Larsen RA, Wood GE, Postle K.** 1993. The conserved proline-rich motif is not essential for energy transduction by *Escherichia coli* TonB protein. Mol Microbiol **10:**943-953.

25. **Skare JT, Roof SK, Postle K.** 1989. A mutation in the amino terminus of a hybrid TrpC-TonB protein relieves overproduction lethality and results in cytoplasmic accumulation. J. Bacteriol. **171:**4442-4447.

bioRxiv preprint doi: https://doi.org/10.1101/2021.12.08.471779; this version posted December 8, 2021. The copyright holder for this preprint (which was not certified by peer review) is the author/funder. All rights reserved. No reuse allowed without permission.

980 26. **Vakharia-Rao H, Kastead KA, Savenkova MI, Bulathsinghala CM,**
981 **Postle K.** 2007. Deletion and substitution analysis of the *Escherichia coli* TonB
982 Q160 region. J. Bacteriol. **189:**4662-4670.
983 27. **Postle K, Kastead KA, Gresock MG, Ghosh J, Swayne CD.** 2010. The
984 TonB dimeric crystal structures do not exist *in vivo*. mBio **1:**e00307-00310.
985 28. **Swayne C, Postle K.** 2011. Taking the *Escherichia coli* TonB
986 transmembrane domain "Offline"? Non-protonatable Asn substitutes fully for
987 TonB His20. J. Bacteriol. **193:**3693-3701.
988 29. **Ghosh J, Postle K.** 2004. Evidence for dynamic clustering of carboxy-
989 terminal aromatic amino acids in TonB-dependent energy transduction. Mol.
990 Microbiol. **51:**203-213.
991 30. **Cascales E, Buchanan SK, Duché D, Kleanthous C, Lloubes R, Postle K,**
992 **Riley M, Slatin S, Cavard D.** 2007. Colicin Biology. Micro. Mol. Biol. Rev.
993 **71:**158-229.
994 31. **Gresock MG, Kastead KA, Postle K.** 2015. From homodimer to
995 heterodimer and back: Elucidating the TonB energy transduction cycle. J.
996 Bacteriol. **197:**3433-3445.
997 32. **Higgs PI, Larsen RA, Postle K.** 2002. Quantitation of known components
998 of the *Escherichia coli* TonB-dependent energy transduction system: TonB, ExbB,
999 ExbD, and FepA. Mol. Microbiol. **44:**271-281.

bioRxiv preprint doi: https://doi.org/10.1101/2021.12.08.471779; this version posted December 8, 2021. The copyright holder for this preprint (which was not certified by peer review) is the author/funder. All rights reserved. No reuse allowed without permission.

33. **Kadner RJ, Heller KJ.** 1995. Mutual inhibition of cobalamin and siderophore uptake systems suggests their competition for TonB function. J. Bacteriol. **177:**4829-4835.

34. **Ollis AA, Postle K.** 2011. The same periplasmic ExbD residues mediate *in vivo* interactions between ExbD homodimers and ExbD-TonB heterodimers. J. Bacteriol. **193:**6852-6863.

35. **Ollis AA, Postle K.** 2012. Identification of functionally important TonB-ExbD periplasmic domain interactions *in vivo*. J. Bacteriol. **194:**3078-3087.

36. **Endriss F, Braun M, Killmann H, Braun V.** 2003. Mutant analysis of the *Escherichia coli* FhuA protein reveals sites of FhuA activity. J. Bacteriol. **185:**4683-4692.

37. **Larsen RA, FosterHartnett D, McIntosh MA, Postle K.** 1997. Regions of *Escherichia coli* TonB and FepA proteins essential for *in vivo* physical interactions. J. Bacteriol. **179:**3213-3221.

38. **Evans JS, Levine BA, Trayer IP, Dorman CJ, Higgins CF.** 1986. Sequence-imposed structural constraints in the TonB protein of *E. coli*. FEBS Lett. **208:**211-216.

39. **Seliger SS, Mey AR, Valle AM, Payne SM.** 2001. The two TonB systems of *Vibrio cholerae*: redundant and specific functions. Mol. Microbiol. **39:**801-812.

bioRxiv preprint doi: https://doi.org/10.1101/2021.12.08.471779; this version posted December 8, 2021. The copyright holder for this preprint (which was not certified by peer review) is the author/funder. All rights reserved. No reuse allowed without permission.

40. **Gresock MG, Postle K.** 2017. Going outside the TonB Box: Identification of novel FepA-TonB interactions *in vivo*. J. Bacteriol. **199:**e00649-00616.

41. **Postle K, Good RF.** 1983. DNA sequence of the *Escherichia coli tonB* gene. Proc. Natl. Acad. Sci. USA **80:**5235-5239.

42. **Larsen RA, Chen GJ, Postle K.** 2003. Performance of standard phenotypic assays for TonB activity, as evaluated by varying the level of functional, wild-type TonB. J. Bacteriol. **185:**4699-4706.

43. **Letain TE, Postle K.** 1997. TonB protein appears to transduce energy by shuttling between the cytoplasmic membrane and the outer membrane in Gram-negative bacteria. Mol. Microbiol. **24:**271-283.

44. **Larsen RA, Deckert GE, Kastead KA, Devanathan S, Keller KL, Postle K.** 2007. His20 provides the sole functionally significant side chain in the essential TonB transmembrane domain. J. Bacteriol. **189:**2825-2833.

45. **Shultis DD, Purdy MD, Banchs CN, Wiener MC.** 2006. Outer membrane active transport: structure of the BtuB:TonB complex. Science **312:**1396-1399.

46. **Kaserer WA, Jiang X, Xiao Q, Scott DC, Bauler M, Copeland D, Newton SM, Klebba PE.** 2008. Insight from TonB hybrid proteins into the mechanism of iron transport through the outer membrane. J. Bacteriol. **190:**4001-4016.

bioRxiv preprint doi: https://doi.org/10.1101/2021.12.08.471779; this version posted December 8, 2021. The copyright holder for this preprint (which was not certified by peer review) is the author/funder. All rights reserved. No reuse allowed without permission.

1038 47. **Higgs PI, Letain TE, Merriam KK, Burke NS, Park H, Kang C, Postle**
1039 **K.** 2002. TonB interacts with nonreceptor proteins in the outer membrane of
1040 *Escherichia coli*. J. Bacteriol. **184:**1640-1648.
1041 48. **Heller KJ, Kadner RJ, Günter K.** 1988. Suppression of the *btuB*451
1042 mutation by mutations in the *tonB* gene suggests a direct interaction between TonB
1043 and TonB-dependent receptor proteins in the outer membrane of *Escherichia coli*.
1044 Gene **64:** 147-153.
1045 49. **Bell PE, Nau CD, Brown JT, Konisky J, Kadner RJ.** 1990. Genetic
1046 suppression demonstrates direct interaction of TonB protein with outer membrane
1047 transport proteins in *Escherichia coli*. J. Bacteriol. **172:**3826-3829.
1048 50. **Cadieux N, Bradbeer C, Kadner RJ.** 2000. Sequence changes in the ton
1049 box region of BtuB affect its transport activities and interaction with TonB protein.
1050 J. Bacteriol. **182:**5954-5961.
1051 51. **Mende J, Braun V.** 1990. Import-defective colicin B derivatives mutated in
1052 the TonB box. Mol. Microbiol. **4:**1523-1533.
1053 52. **Majumdar A, Trinh V, Moore KJ, Smallwood CR, Kumar A, Yang T,**
1054 **Scott DC, Long NJ, Newton SM, Klebba PE.** 2020. Conformational
1055 rearrangements in the N-domain of *Escherichia coli* FepA during ferric
1056 enterobactin transport. J. Biol. Chem. **295:**4974-4984.

bioRxiv preprint doi: https://doi.org/10.1101/2021.12.08.471779; this version posted December 8, 2021. The copyright holder for this preprint (which was not certified by peer review) is the author/funder. All rights reserved. No reuse allowed without permission.

53. **Chimento DP, Kadner RJ, Wiener MC.** 2005. Comparative structural analysis of TonB-dependent outer membrane transporters: implications for the transport cycle. Proteins **59:**240-251.

54. **Chakraborty R, Storey E, van der Helm D.** 2006. Molecular mechanism of ferricsiderophore passage through the outer membrane receptor proteins of Escherichia coli. Biometals **20:**263-274.

55. **Barnard TJ, Watson ME, Jr., McIntosh MA.** 2001. Mutations in the *Escherichia coli* receptor FepA reveal residues involved in ligand binding and transport. Mol. Microbiol. **41:**527-536.

56. **Carter DM, Gagnon JN, Damlaj M, Mandava S, Makowski L, Rodi DJ, Pawelek PD, Coulton JW.** 2006. Phage display reveals multiple contact sites between FhuA, an outer membrane receptor of *Escherichia coli*, and TonB. J. Mol. Biol. **357:**236-251.

57. **Nilaweera TD, Nyenhuis DA, Cafiso DS.** 2021. Structural intermediates observed only in intact Escherichia coli indicate a mechanism for TonB-dependent transport. Elife **10:**e68548.

58. **Larsen RA, Letain TE, Postle K.** 2003. *In vivo* evidence of TonB shuttling between the cytoplasmic and outer membrane in *Escherichia coli*. Mol. Microbiol. **49:**211-218.

bioRxiv preprint doi: https://doi.org/10.1101/2021.12.08.471779; this version posted December 8, 2021. The copyright holder for this preprint (which was not certified by peer review) is the author/funder. All rights reserved. No reuse allowed without permission.

59. **Bitter W, Tommassen J, Weisbeek PJ.** 1993. Identification and characterization of the *exbB*, *exbD* and *tonB* Genes of *Pseudomonas putida* WCS358 - Their involvement in ferric pseudobactin transport. Mol. Microbiol. **7:**117-130.

60. **Buchanan SK, Smith BS, Venkatramani L, Xia D, Esser L, Palnitkar M, Chakraborty R, van der Helm D, Deisenhofer J.** 1999. Crystal structure of the outer membrane active transporter FepA from *Escherichia coli*. Nat. Struct. Biol. **6:**56-63.

61. **Hilsenbeck JL, Park H, Chen G, Youn B, Postle K, Kang C.** 2004. Crystal structure of the cytotoxic bacterial protein colicin B at 2.5 A resolution. Mol. Microbiol. **51:**711-720.

62. **White P, Joshi A, Rassam P, Housden NG, Kaminska R, Goult JD, Redfield C, McCaughey LC, Walker D, Mohammed S, Kleanthous C.** 2017. Exploitation of an iron transporter for bacterial protein antibiotic import. Proc. Natl. Acad. Sci. USA **114:**12051-12056.

63. **Hullmann J, Patzer SI, Romer C, Hantke K, Braun V.** 2008. Periplasmic chaperone FkpA is essential for imported colicin M toxicity. Mol. Microbiol. **69:**926-937.

64. **Landeta C, Boyd D, Beckwith J.** 2018. Disulfide bond formation in prokaryotes. Nat. Microbiol. **3:**270-280.

bioRxiv preprint doi: https://doi.org/10.1101/2021.12.08.471779; this version posted December 8, 2021. The copyright holder for this preprint (which was not certified by peer review) is the author/funder. All rights reserved. No reuse allowed without permission.

65. **Kopp DR, Postle K.** 2020. The intrinsically disordered region of ExbD is required for signal transduction. J. Bacteriol. **202:**e00687-00619.

66. **Mann BJ, Holroyd CD, Bradbeer C, Kadner RJ.** 1986. Reduced activity of TonB-dependent functions in strains of *Escherichia coli*. *FEMS Lett.* **33:**255-260.

67. **Larsen RA, Thomas MG, Postle K.** 1999. Protonmotive force, ExbB and ligand-bound FepA drive conformational changes in TonB. Mol. Microbiol. **31:**1809-1824.

68. **Lee SK, Keasling JD.** 2005. A propionate-inducible expression system for enteric bacteria. Appl. Environ. Microbiol. **71:**6856-6862.

69. **Postle K.** 2007. TonB system, *in vivo* assays and characterization. Methods Enzymol. **422:**245-269.

70. **Laemmli UK.** 1970. Cleavage of structural proteins during the assembly of the head of bacteriophage T4. Nature **227:**680-685.

71. **Larsen RA, Myers PS, Skare JT, Seachord CL, Darveau RP, Postle K.** 1996. Identification of TonB homologs in the family *Enterobacteriaceae* and evidence for conservation of TonB-dependent energy transduction complexes. J. Bacteriol. **178:**1363-1373.

72. **Skare JT, Postle K.** 1991. Evidence for a TonB-dependent energy transduction complex in *Escherichia coli*. Mol. Microbiol. **5:**2883-2890.

bioRxiv preprint doi: https://doi.org/10.1101/2021.12.08.471779; this version posted December 8, 2021. The copyright holder for this preprint (which was not certified by peer review) is the author/funder. All rights reserved. No reuse allowed without permission.

73. **Hill CW, Harnish BW.** 1981. Inversions between ribosomal RNA genes of *Escherichia coli*. Proc. Natl. Acad. Sci. USA **78:**7069-7072.

74. **Baker KR, Postle K.** 2013. Mutations in *Escherichia coli* ExbB transmembrane domains identify scaffolding and signal transduction functions and exclude participation in a proton pathway. J. Bacteriol. **195:**2898-2911.

75. **Chang C, Mooser A, Pluckthun A, Wlodawer A.** 2001. Crystal structure of the dimeric C-terminal domain of TonB reveals a novel fold. J. Biol. Chem. **276:**27535-27540.

76. **Peacock SR, Weljie AM, Peter Howard S, Price FD, Vogel HJ.** 2005. The solution structure of the C-terminal domain of TonB and interaction studies with TonB box peptides. J. Mol. Biol. **345:**1185-1197.

77. **Symmons MF, Bokma E, Koronakis E, Hughes C, Koronakis V.** 2009. The assembled structure of a complete tripartite bacterial multidrug efflux pump. Proc. Natl. Acad. Sci. USA **106:**7173-7178.

78. **Drozdetskiy A, Cole C, Procter J, Barton GJ.** 2015. JPred4: a protein secondary structure prediction server. Nucl. Acids Res. **43:**W389-394.

bioRxiv preprint doi: https://doi.org/10.1101/2021.12.08.471779; this version posted December 8, 2021. The copyright holder for this preprint (which was not certified by peer review) is the author/funder. All rights reserved. No reuse allowed without permission.

# TABLES

**Table 1**: [$^{55}$Fe]-enterochelin transport activities of TonB and FepA Cys substitutions

| Mutant | Percent activity (%) relative to "wild-type" |
|---|---|
| TonB C18G | 100 |
| TonB C18G Q160C | 113 |
| TonB C18G M201C | 95 |
| TonB C18G R204C | 107 |
| TonB C18G V206C | 71 |
| TonB C18G N208C | 76 |
| TonB C18G A209C | 65 |
| TonB C18G R212C | 96 |
| TonB C18G R214C | 75 |
| TonB C18G H20A Q160C | 5 |
| TonB C18G H20A M201C | 3 |
| TonB C18G H20A R204C | 3 |
| TonB C18G H20A N208C | 1 |
| TonB C18G H20A R212C | 2 |
| TonB C18G H20A R214C | 2 |
| FepA wild-type | 100 |

bioRxiv preprint doi: https://doi.org/10.1101/2021.12.08.471779; this version posted December 8, 2021. The copyright holder for this preprint (which was not certified by peer review) is the author/funder. All rights reserved. No reuse allowed without permission.

| | |
|---|---|
| FepA V16C | 91 |
| FepA L23C | 79 |
| FepA S29C | 98 |
| FepA T32C | 92 |
| FepA A33C | 89 |
| FepA D34C | 115 |
| FepA E35C | 86 |
| FepA A42C | 77 |
| FepA S46C | 76 |
| FepA T51C | 85 |
| FepA G54C | 86 |
| FepA R75C | 40 |
| FepA L85C | 107 |
| FepA V91C | 84 |
| FepA S92C | 101 |
| FepA S112C | 105 |
| FepA E120C | 83 |
| FepA V124C | 102 |
| FepA R126C | 46 |
| FepA A131C | 72 |

bioRxiv preprint doi: https://doi.org/10.1101/2021.12.08.471779; this version posted December 8, 2021. The copyright holder for this preprint (which was not certified by peer review) is the author/funder. All rights reserved. No reuse allowed without permission.

| | |
|---|---|
| FepA V142C | 78 |
| FepA I145C | 84 |
| FepA E152C | 62 |
| FepA D185C | 118 |
| FepA P243C | 106 |
| FepA D298C | 126 |
| FepA D356C | 115 |
| FepA D422C | 109 |
| FepA D455C | 121 |
| FepA E511C | 92 |
| FepA D519C | 136 |
| FepA E567C | 65 |
| FepA E576C | 134 |
| FepA D618C | 104 |
| FepA D664C | 105 |
| FepA T722C | 60 |

1135

1136

1137

bioRxiv preprint doi: https://doi.org/10.1101/2021.12.08.471779; this version posted December 8, 2021. The copyright holder for this preprint (which was not certified by peer review) is the author/funder. All rights reserved. No reuse allowed without permission.

1138 **Table 2**: Strains and plasmids

| Strain or plasmid | Genotype | Reference |
|---|---|---|
| Strains | | |
| DH5α | F- Φ80d/*acZ*ΔM15 Δ(*lacZYA-argF)* U169 *deoR recA1 endA1 hsdR17* (rk-, mk+) *phoA supE44* I- thi-1 *gyrA96 relA1* | Life Technologies |
| W3110 | F- IN(*rrnD-rrnE)1* | (73) |
| KP1270 | W3110 *aroB* | (67) |
| KP1344 | W3110 Δ(*tonB, P14)::blaM* | (67) |
| KP1406 | W3110 *aroB* Δ(*tonB, P14)::blaM* | (11) |
| KP1477 | W3110 Δ(*tonB, P14)::kan* | (12) |
| KP1487 | W3110 Δ*fepA::kan* | (40) |
| KP1489 | W3110 Δ*fepA,* a derivative of KP1487 | (40) |
| KP1490 | W3110 *aroB* Δ*fepA* | (12) |
| KP1491 | W3110 Δ*fepA* (*tonB, P14)::kan* | Present study |
| RA1021 | W3110 Δ*exbD* | (18) |
| TonB Plasmids | | |
| pKP325 | Wild-type TonB in pACYC184 | (67) |
| pKP372 | TonB amphipathic helix frameshift in pKP325 | Present study |
| pKP1859 | pKP372, C18G | Present study |

bioRxiv preprint doi: https://doi.org/10.1101/2021.12.08.471779; this version posted December 8, 2021. The copyright holder for this preprint (which was not certified by peer review) is the author/funder. All rights reserved. No reuse allowed without permission.

| | | |
|---|---|---|
| pKP442 | Wild-type TonB in pKP325, silent XhoI site | (29) |
| pKP568 | pKP442 with TonB C18G | (29) |
| pKP531 | pKP442 with TonB F202A, W213A | (29) |
| pKP532 | pKP442 with TonB F202A, Y215A | (29) |
| pKP476 | pKP442 with TonB Δ199-216 | Present study |
| pKP1858 | pKP476, C18G | Present study |
| pKP1362 | TonB C18G in pPro33 | Present study |
| pKP1427 | TonB C18G Q160C, a derivative of pKP1362 | Present study |
| pKP2303 | TonB C18G Q160C F202A, a derivative of pKP1427 | Present study |
| pKP2304 | TonB C18G Q160C F202A W213A, a derivative of pKP2303 | Present study |
| pKP1676 | TonB C18G M201C, a derivative of pKP1362 | Present study |
| pKP1867 | TonB C18G R204C, a derivative of pKP1362 | Present study |
| pKP1683 | TonB C18G V206C, a derivative of pKP1362 | Present study |
| pKP1646 | TonB C18G N208C, a derivative of pKP1362 | Present study |
| pKP1647 | TonB C18G A209C, a derivative of pKP1362 | Present study |
| pKP1624 | TonB C18G R212C, a derivative of pKP1362 | Present study |
| pKP1684 | TonB C18G R214C, a derivative of pKP1362 | Present study |
| pKP1708 | TonB C18G H20A Q160C, a derivative of pKP1427 | Present study |
| pKP1720 | TonB C18G H20A M201C, a derivative of pKP1676 | Present study |

bioRxiv preprint doi: https://doi.org/10.1101/2021.12.08.471779; this version posted December 8, 2021. The copyright holder for this preprint (which was not certified by peer review) is the author/funder. All rights reserved. No reuse allowed without permission.

| | | |
|---|---|---|
| pKP1868 | TonB C18G H20A R204C, a derivative of pKP1645 | Present study |
| pKP1722 | TonB C18G H20A V206C, a derivative of pKP1683 | Present study |
| pKP1692 | TonB C18G H20A N208C, a derivative of pKP1646 | Present study |
| pKP2299 | TonB C18G H20A V209C, a derivative of pKP1647 | Present study |
| pKP1861 | TonB C18G H20A R212C, a derivative of pKP1624 | Present study |
| pKP1723 | TonB C18G H20A R214C, a derivative of pKP1684 | Present study |

FepA plasmids

| | | |
|---|---|---|
| pKP515 | WT FepA in pBAD24 | (11) |
| pKP1410 | FepA D12C, a pKP515 derivative | Present study |
| pKP718 | FepA T13C, a pKP515 derivative | (12) |
| pKP1411 | FepA I14C, a pKP515 derivative | Present study |
| pKP1383 | FepA V15C, a pKP515 derivative | Present study |
| pKP1384 | FepA V16C, a pKP515 derivative | Present study |
| pKP1416 | FepA T17C, a pKP515 derivative | Present study |
| pKP1626 | FepA D34C, ΔTonB box (residues 12-16), derivative of pKP1583 | Present study |
| pKP1627 | FepA G54C, ΔTonB box (residues 12-16), derivative of pKP1382 | Present study |
| pKP1582 | FepA L23C, a pKP515 derivative | Present study |

bioRxiv preprint doi: https://doi.org/10.1101/2021.12.08.471779; this version posted December 8, 2021. The copyright holder for this preprint (which was not certified by peer review) is the author/funder. All rights reserved. No reuse allowed without permission.

| | | |
|---|---|---|
| pKP719 | FepA S29C, a pKP515 derivative | (12) |
| pKP1577 | FepA T32C, a pKP515 derivative | Present study |
| pKP728 | FepA A33C, a pKP515 derivative | (12) |
| pKP1583 | FepA D34C, a pKP515 derivative | Present study |
| pKP1578 | FepA E35C, a pKP515 derivative | Present study |
| pKP720 | FepA A42C, a pKP515 derivative | (12) |
| pKP729 | FepA S46C, a pKP515 derivative | (12) |
| pKP730 | FepA T51C, a pKP515 derivative | (12) |
| pKP1382 | FepA G54C, a pKP515 derivative | Present study |
| pKP1400 | FepA R75C, a pKP515 derivative | Present study |
| pKP1581 | FepA L85C, a pKP515 derivative | Present study |
| pKP731 | FepA V91C, a pKP515 derivative | (12) |
| pKP721 | FepA S92C, a pKP515 derivative | (12) |
| pKP732 | FepA S112C, a pKP515 derivative | (12) |
| pKP1836 | FepA E120C, a pKP515 derivative | Present study |
| pKP733 | FepA V124C, a pKP515 derivative | (12) |
| pKP1506 | FepA R126C, a pKP515 derivative | Present study |
| pKP1854 | FepA A131C, a pKP515 derivative | Present study |
| pKP1841 | FepA V142C, a pKP515 derivative | Present study |
| pKP1837 | FepA I145C, a pKP515 derivative | Present study |

bioRxiv preprint doi: https://doi.org/10.1101/2021.12.08.471779; this version posted December 8, 2021. The copyright holder for this preprint (which was not certified by peer review) is the author/funder. All rights reserved. No reuse allowed without permission.

| | | |
|---|---|---|
| pKP1857 | FepA E152C, a pKP515 derivative | Present study |
| pKP1369 | FepA D185C, a pKP515 derivative | Present study |
| pKP1864 | FepA P243C, a pKP515 derivative | Present study |
| pKP1361 | FepA D298C, a pKP515 derivative | Present study |
| pKP1685 | FepA D356C, a pKP515 derivative | Present study |
| pKP1726 | FepA D422C, a pKP515 derivative | Present study |
| pKP1656 | FepA D455C, a pKP515 derivative | Present study |
| pKP1609 | FepA E511C, a pKP515 derivative | Present study |
| pKP1410 | FepA D519C, a pKP515 derivative | Present study |
| pKP1610 | FepA E567C, a pKP515 derivative | Present study |
| pKP1793 | FepA E576C, a pKP515 derivative | Present study |
| pKP1370 | FepA D618C, a pKP515 derivative | Present study |
| pKP1727 | FepA D664C, a pKP515 derivative | Present study |
| pKP1850 | FepA T722C, a pKP515 derivative | Present study |

1139

bioRxiv preprint doi: https://doi.org/10.1101/2021.12.08.471779; this version posted December 8, 2021. The copyright holder for this preprint (which was not certified by peer review) is the author/funder. All rights reserved. No reuse allowed without permission.

# FIGURES

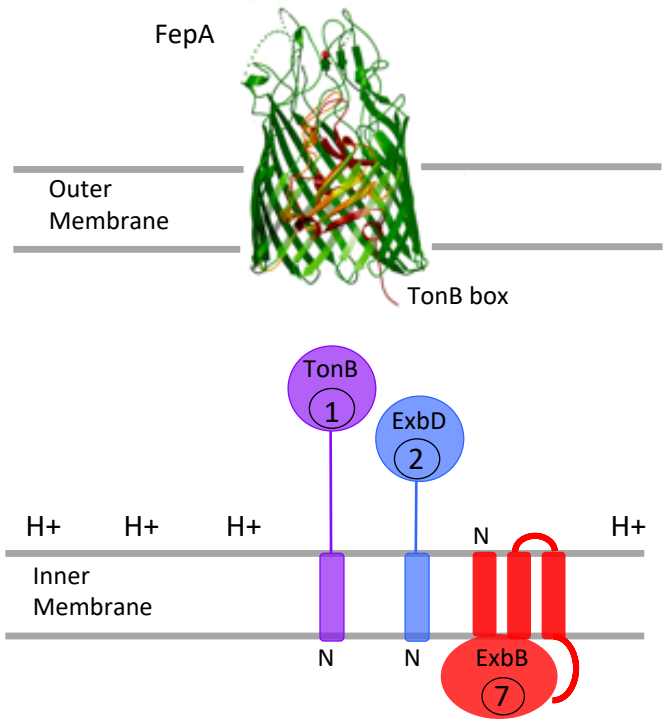


**Figure 1. The TonB system of *Escherichia coli* K12.** The TonB-dependent transporter, FepA, is shown in the outer membrane. At its extreme amino terminus, the TonB box, the only known site of *in vivo* interaction with TonB, is shown protruding into the periplasm. The topologies and cellular ratios of the cytoplasmic membrane proteins TonB, ExbB and ExbD are shown in the cytoplasmic membrane. The protonmotive force gradient of the cytoplasmic membrane (H+) is shown. The crystal structure of FepA was solved by Buchanan et al. (60).

bioRxiv preprint doi: https://doi.org/10.1101/2021.12.08.471779; this version posted December 8, 2021. The copyright holder for this preprint (which was not certified by peer review) is the author/funder. All rights reserved. No reuse allowed without permission.

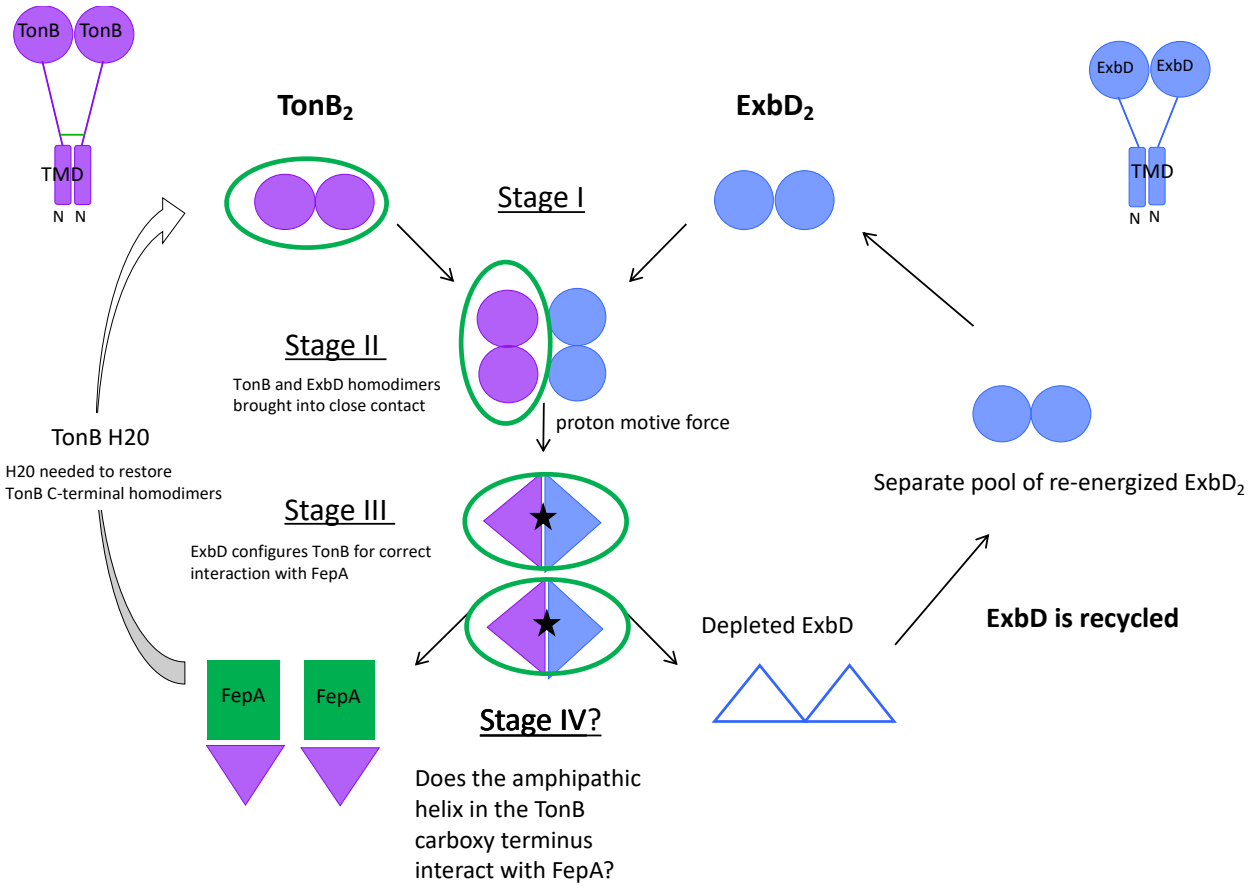


**Figure 2. Key *in vivo* interactions of the TonB carboxy terminus during the energy transduction cycle involve the amphipathic helix (residues 199-216) [adapted from (31).].** Full length TonB (purple, upper left corner) and ExbD (blue, upper right corner) each have a single transmembrane domain signal anchor in the cytoplasmic membrane with the bulk of the residues occupying the periplasmic space. Filled purple circles/triangles are TonB carboxy termini. Filled blue circles/triangles are ExbD carboxy termini. The TonB amino terminal domain remains homodimerized throughout the cycle, with its periplasmic carboxy

bioRxiv preprint doi: https://doi.org/10.1101/2021.12.08.471779; this version posted December 8, 2021. The copyright holder for this preprint (which was not certified by peer review) is the author/funder. All rights reserved. No reuse allowed without permission.

terminus undergoing sequential protein-protein interactions (31). Interactions of the periplasmic carboxy-terminal domains of both $TonB_2$ and $ExbD_2$ homodimers are shown. In Stage I, H20 in the TonB transmembrane domain is required for TonB carboxy termini to form obligatory homodimers through residues in and near the carboxy terminal amphipathic helix (residues 199-216), (17, 31). ExbB tetramers ($ExbB_4$) independently stabilize both $TonB_2$ and $ExbD_2$, homodimerized through their carboxy termini, and are proposed to be the scaffolds upon which $TonB_2$ and $ExbD_2$ are independently assembled ($ExbB_4$ is not shown). In Stage II, $TonB_2$ and $ExbD_2$ homodimers are brought into close contact by ExbB tetramers but have not yet formed the heterodimers of the subsequent Stage. In Stage III, in the presence of the cytoplasmic membrane protonmotive force (PMF), the $TonB_2$ and $ExbD_2$ carboxy termini reassort to form two TonB-ExbD heterodimers. ExbD, which contains the sole potentially PMF-responsive residue (Asp25) among five transmembrane domains that make up the TonB system, configures TonB correctly for a productive interaction with FepA [(28, 74); Jana and Postle, unpublished]. This is necessary because inactive TonB also binds to TBDTs but without energy transduction, meaning that the correct configuration must be based on prior interaction with ExbD. Stage IV is binding of a monomeric carboxy terminus of TonB to FepA, such that active transport of the siderophore enterochelin across the outer membrane occurs. Notably, the TonB amphipathic helix makes important

bioRxiv preprint doi: https://doi.org/10.1101/2021.12.08.471779; this version posted December 8, 2021. The copyright holder for this preprint (which was not certified by peer review) is the author/funder. All rights reserved. No reuse allowed without permission.

contacts with another TonB or ExbD in Stages I-III (green circles), however it has never been tested for important contacts with FepA (green square). After a transport event, H20 is required for re-formation of TonB dimers in Stage I. $ExbD_2$ is de-energized after this event (empty blue triangles) and needs to be recycled. We speculate that $ExbD_2$ moves in and out of the complex escorted by ExbB tetramers. A separate pool of recycled $ExbB_4$-$ExbD_2$ is hypothesized to exist to replenish Stage I $ExbB_4$-ExbD homodimers. See (31) for a full explanation of the experimental basis for the model.

bioRxiv preprint doi: https://doi.org/10.1101/2021.12.08.471779; this version posted December 8, 2021. The copyright holder for this preprint (which was not certified by peer review) is the author/funder. All rights reserved. No reuse allowed without permission.

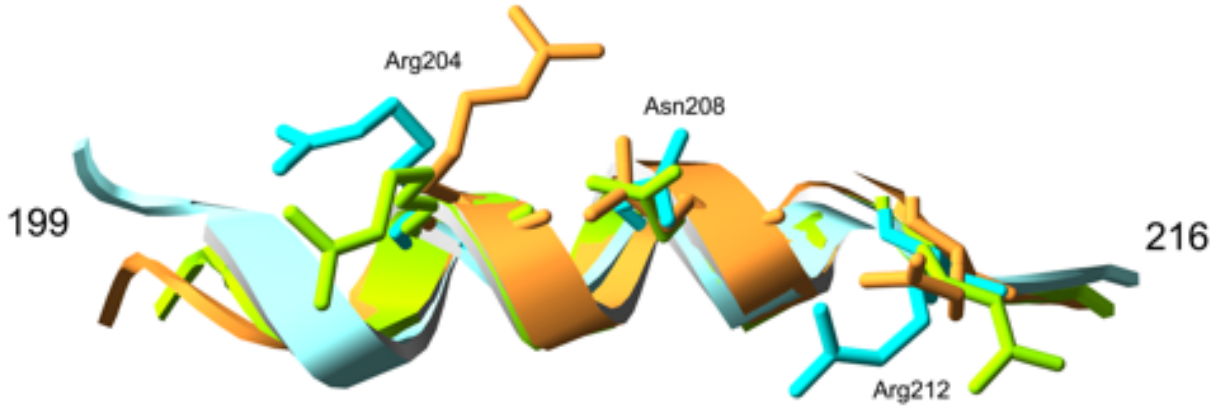


**Figure 3. Superimposition of the TonB amphipathic helices from TonB crystal structures.** Blue is from Chang et al. (75); green is from Peacock et al. (76); gold is from Shultis et al. (45). The hydrophilic residues that, as Cys substitutions, interact with the FepA TonB box Cys substitutions in Fig. 7 are shown.

bioRxiv preprint doi: https://doi.org/10.1101/2021.12.08.471779; this version posted December 8, 2021. The copyright holder for this preprint (which was not certified by peer review) is the author/funder. All rights reserved. No reuse allowed without permission.

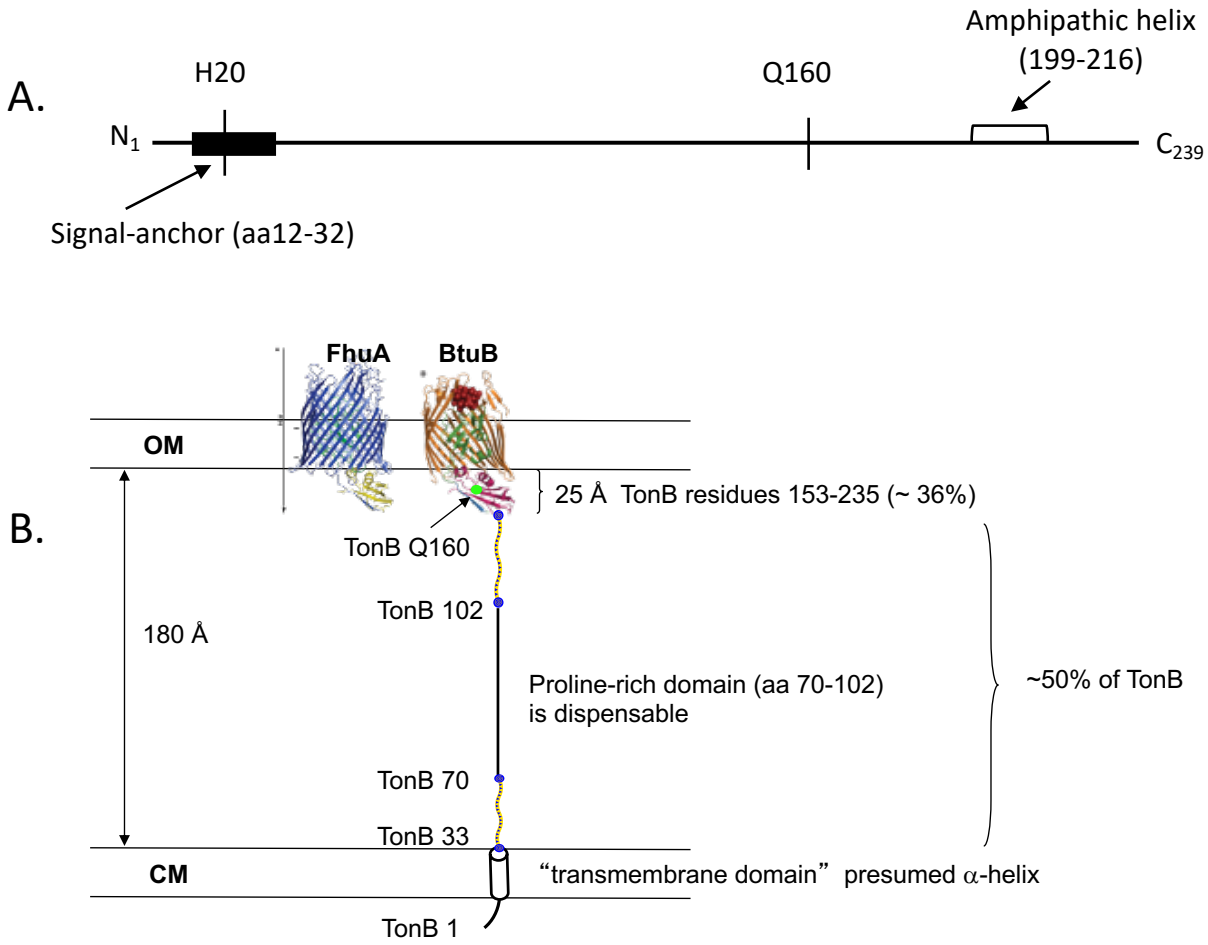


1212

1213

1214 **Figure 4. TonB protein information. (A)** Relevant features of the TonB

1215 primary amino acid sequence (residues 1-239) are shown. H20 in the TonB

1216 transmembrane signal anchor domain renders TonB inactive when substituted with

1217 alanine (44). Locations of TonB Q160 and the amphipathic helix are shown. **(B)**

1218 The conformation of TonB predicted by the crystal structures of its carboxy

1219 terminus would be unable to reach the TBDTs. TonB residues 33–69 and 103–149,

1220 predicted to be intrinsically disordered regions (44) are depicted as yellow

bioRxiv preprint doi: https://doi.org/10.1101/2021.12.08.471779; this version posted December 8, 2021. The copyright holder for this preprint (which was not certified by peer review) is the author/funder. All rights reserved. No reuse allowed without permission.

rectangles. TonB Q160 is the green dot within the structured carboxy terminus of the BtuB-TonB structure. The proline-rich domain, which contributes ~ 100 Å to the extension of TonB across the periplasmic space (38), can be deleted without inactivating TonB (24, 39). The span of the periplasmic space was estimated based on crystal structure reconstructions of the AcrA/B/TolC complex which has proteins in both outer and cytoplasmic membranes (77). The crystal structure of FhuA-TonB is from Pawelek et al. (20). The crystal structure of BtuB-TonB is from Shultis et al. (45). Part B of this figure is from (44). Abbreviations: CM, cytoplasmic membrane; OM, outer membrane.

bioRxiv preprint doi: https://doi.org/10.1101/2021.12.08.471779; this version posted December 8, 2021. The copyright holder for this preprint (which was not certified by peer review) is the author/funder. All rights reserved. No reuse allowed without permission.

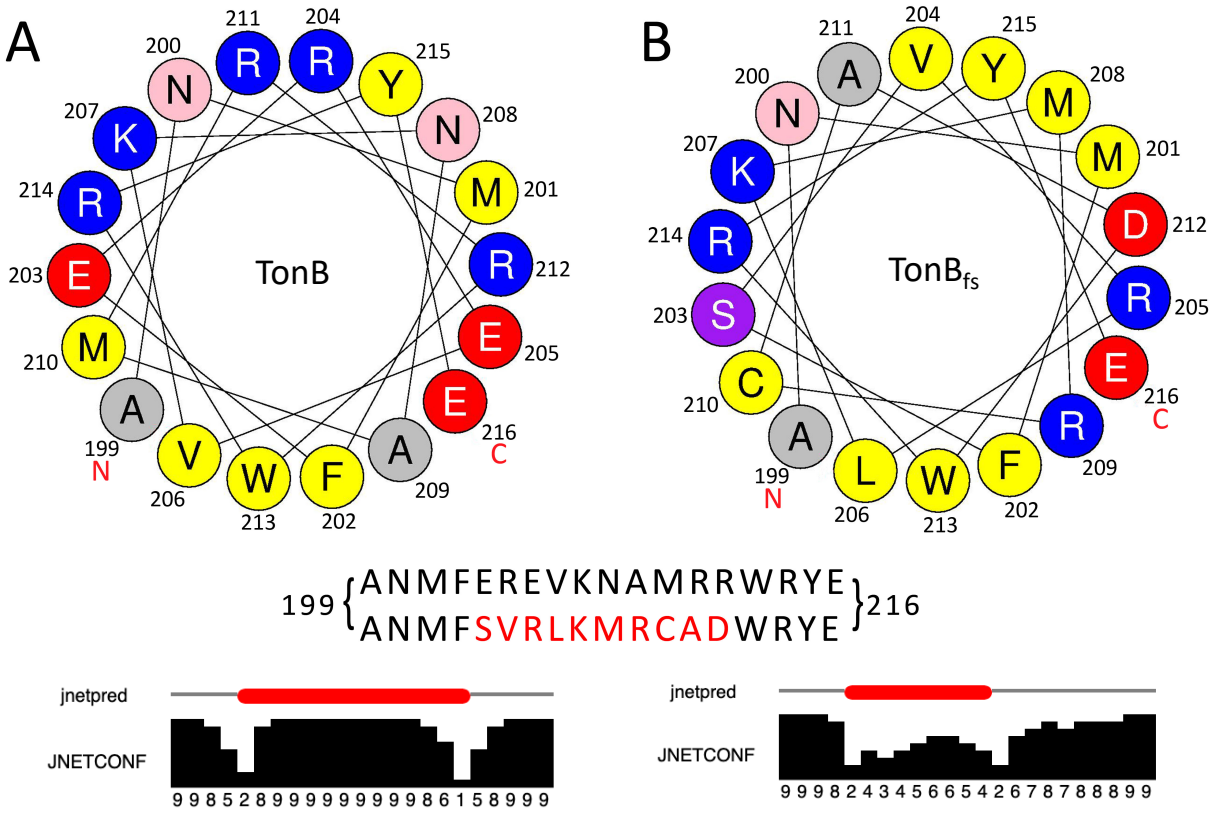


**Figure 5. Comparison of wild type TonB and frame-shifted ($TonB_{fs}$) amphipathic helix regions (residues 199-216).** **(A)** Helical wheel diagram of the TonB amphipathic helix and its corresponding JPRED4 prediction (bottom) as compared to **(B)** the corresponding frame-shifted region of TonB presented in a helical wheel diagram with its corresponding JPRED4 prediction (bottom). For JNetPred, predicted helices are shown in red. For JNETCONF, high values along the bottom edge indicate high confidence in the prediction (78). The comparison of the two amino acid sequences is shown in the middle panel, with the frame-shifted residues noted in red. The frameshifted version has lost much but not all of its

bioRxiv preprint doi: https://doi.org/10.1101/2021.12.08.471779; this version posted December 8, 2021. The copyright holder for this preprint (which was not certified by peer review) is the author/funder. All rights reserved. No reuse allowed without permission.

helical character and it resulted in multiple substitutions in the core helix residues 203-212.

bioRxiv preprint doi: https://doi.org/10.1101/2021.12.08.471779; this version posted December 8, 2021. The copyright holder for this preprint (which was not certified by peer review) is the author/funder. All rights reserved. No reuse allowed without permission.

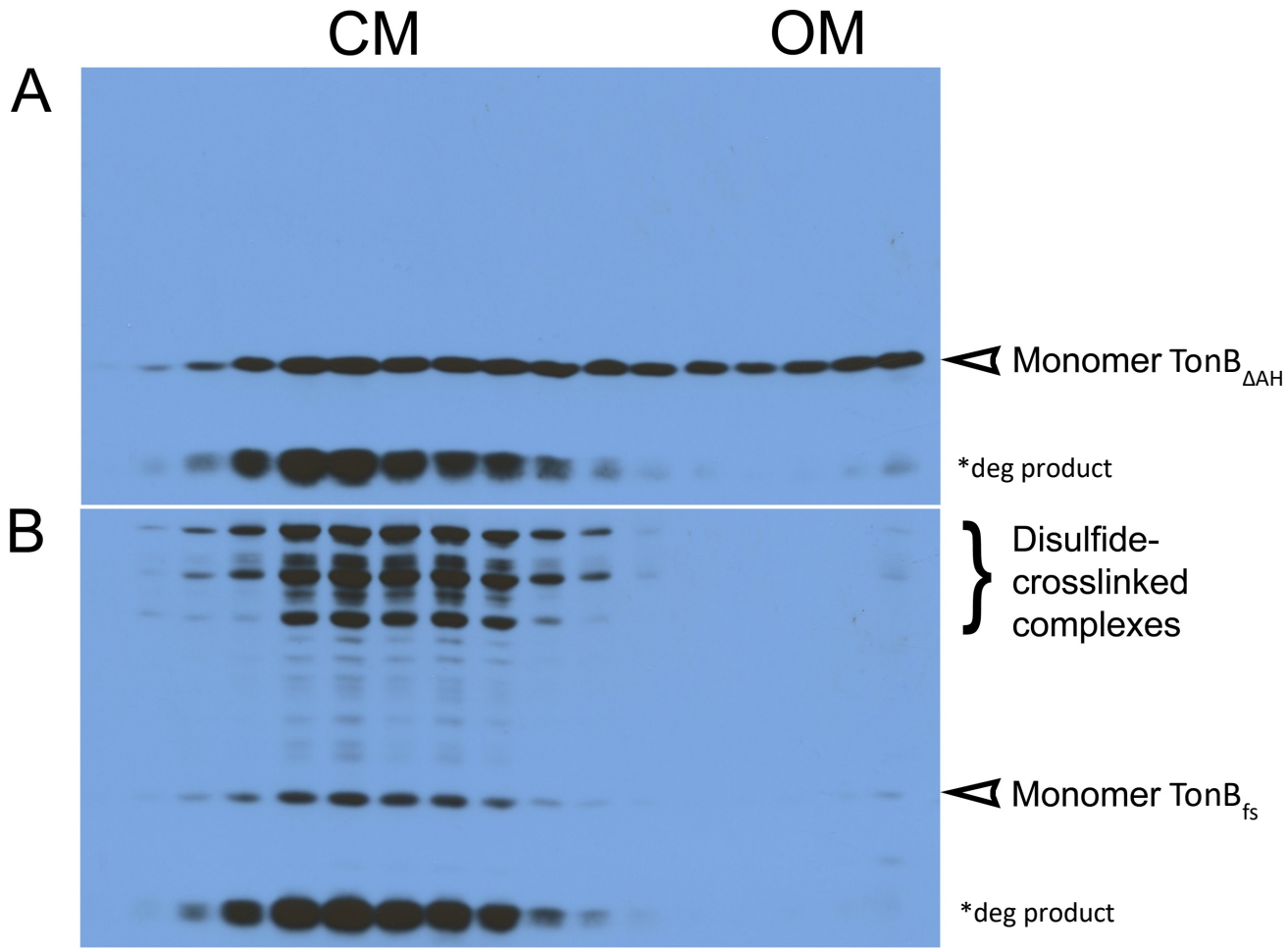


**Figure 6. Monomeric TonB with major alterations of its amphipathic helix retains its ability to associate with the outer membrane.** Wild-type TonB fractionates ~ 40% with the outer membrane and ~ 60% with the cytoplasmic membrane (43). (**A)** Sucrose density gradient fractionation of TonB$_{\Delta AH}$ ,where TonB associates with both membranes. (**B)** Sucrose density gradient fractionation of TonB$_{fs}$ . Because most of the TonB$_{fs}$ is trapped as triplet homodimers through M210C that cannot associate with the outer membrane (17, 31), only a small

bioRxiv preprint doi: https://doi.org/10.1101/2021.12.08.471779; this version posted December 8, 2021. The copyright holder for this preprint (which was not certified by peer review) is the author/funder. All rights reserved. No reuse allowed without permission.

amount of monomer is apparent in OM fractions on this exposure. On longer exposures, monomer $TonB_{fs}$ association with the outer membrane becomes more apparent (data not shown). CM is for cytoplasmic membrane fractions; OM is for outer membrane fractions. Immunoblots of SDS polyacrylamide gels with anti-TonB monoclonal antibody are shown (71).

bioRxiv preprint doi: https://doi.org/10.1101/2021.12.08.471779; this version posted December 8, 2021. The copyright holder for this preprint (which was not certified by peer review) is the author/funder. All rights reserved. No reuse allowed without permission.

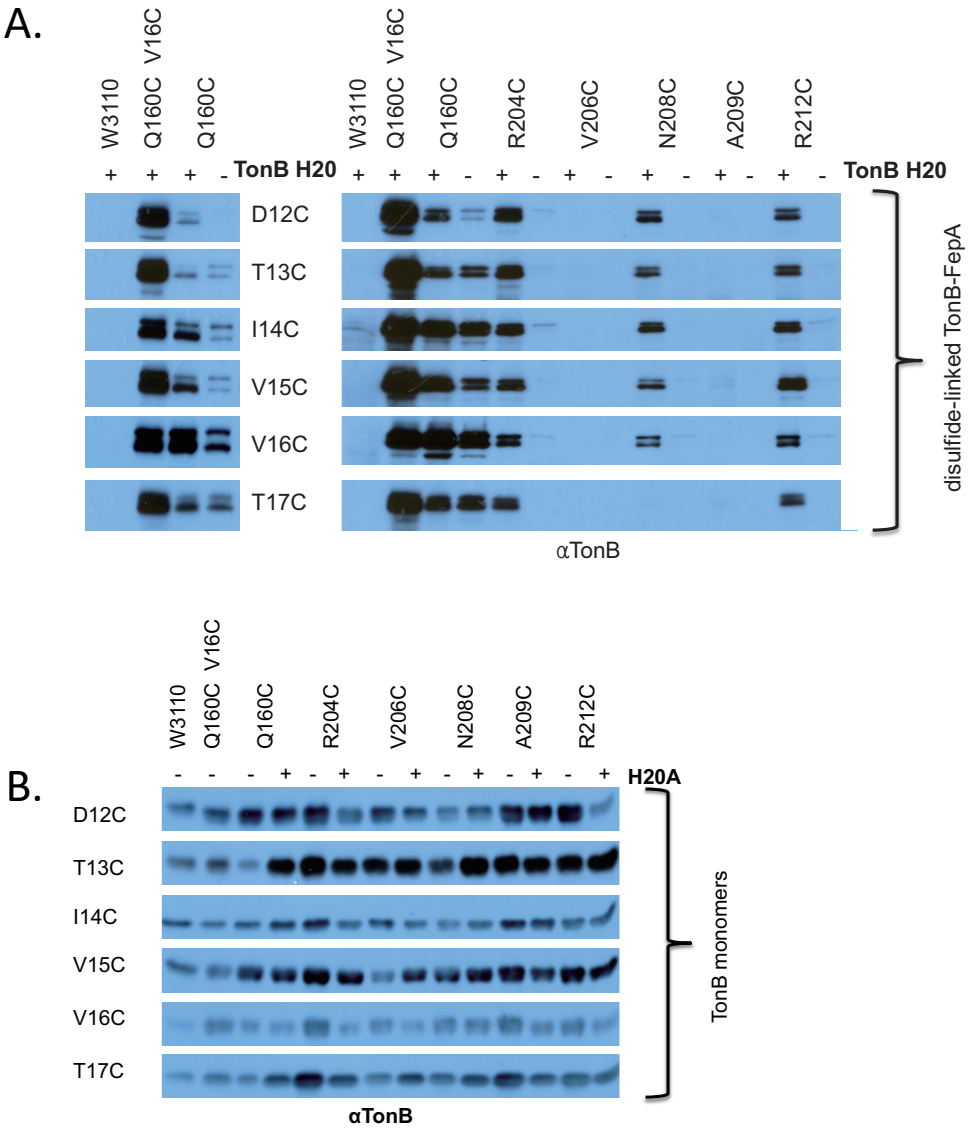


1274

1275 **Fig. 7. Cys substitutions in the essential TonB amphipathic helix form *in vivo***

1276 **disulfide crosslinks with FepA TonB box Cys substitutions.** Strain KP1491

1277 [W3110 Δ*fepA,* Δ(*tonB,P14*)*::kan*] with various TonB and FepA plasmid

1278 combinations was grown and analyzed as described in Materials and Methods.

1279 TonB and its Cys substitutions are indicated across the top of the immunoblots.

bioRxiv preprint doi: https://doi.org/10.1101/2021.12.08.471779; this version posted December 8, 2021. The copyright holder for this preprint (which was not certified by peer review) is the author/funder. All rights reserved. No reuse allowed without permission.

FepA Cys substitutions in the TonB box are indicated between the two panels (in (A) or on the left side of the immunoblot in (B). (+) indicates the presence of the wild-type H20 allele in the TonB transmembrane domain. (-) indicates the presence of the inactivating H20A mutation. Immunoblots of the ~ 116 kDa region of non-reducing SDS polyacrylamide gels developed with monoclonal anti-TonB antibody are shown. (**A)** Wild-type control W3110 shows that wildtype TonB and wildtype FepA do not innately form stable complexes. Panel right: TonB-FepA disulfide-linked complexes are shown. Panel left: shorter exposures of the first four lanes of panel right are shown. In panel left, the TonB Q160C-FepA V16C pair demonstrated the most efficient crosslinking among five TonB FepA TonB box Cys substitutions tested and was therefore used as a standard for relative levels in all subsequent figures characterizing disulfide crosslinks. (**B)** Steady state levels of chromosomally encoded TonB in W3110 and plasmid-encoded TonB variants from samples in (A) are shown as immunoblots of the ~ 36 kDa region of reducing SDS polyacrylamide gels developed with anti-TonB monoclonal antibody.

bioRxiv preprint doi: https://doi.org/10.1101/2021.12.08.471779; this version posted December 8, 2021. The copyright holder for this preprint (which was not certified by peer review) is the author/funder. All rights reserved. No reuse allowed without permission.

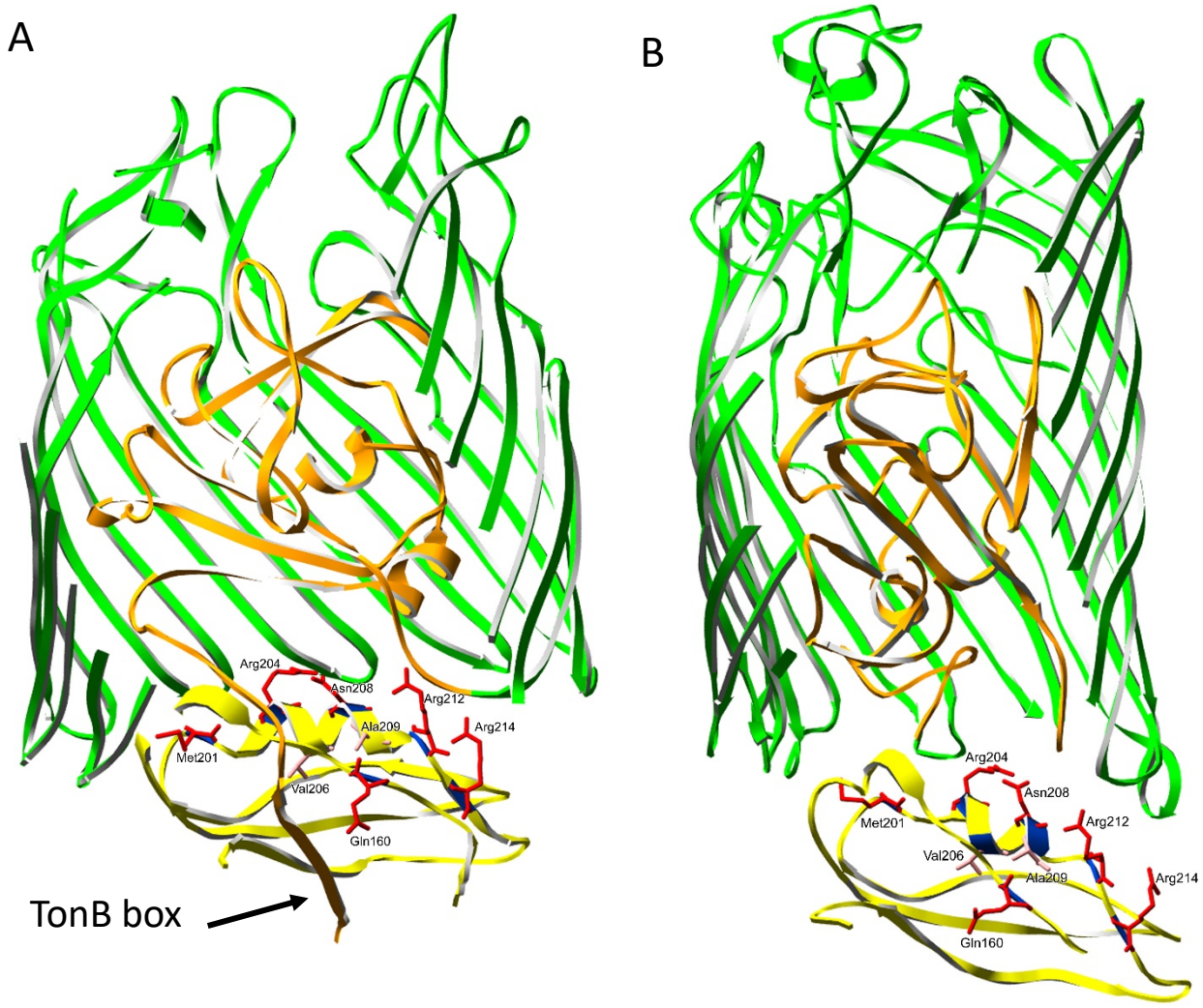


**Figure 8: Ribbon diagrams of TonB Cys-substituted residues displayed on TonB carboxy terminus co-crystal structures with BtuB** [**A**; Shultis et al., (45)] **and FhuA** [**B**; Pawelek et al., (20)]. TonB Cys substitutions from this study that made disulfide crosslinks with a variety of Cys substitutions in FepA, including the TonB box, are in red; those in pink (A206C and A209C) made no crosslinks. The TonB box of BtuB is shown. The FhuA TonB box was not visible in the FhuA-

bioRxiv preprint doi: https://doi.org/10.1101/2021.12.08.471779; this version posted December 8, 2021. The copyright holder for this preprint (which was not certified by peer review) is the author/funder. All rights reserved. No reuse allowed without permission.

TonB structure. The authors of that study propose that FhuA TonB box residues I9, T10, V11, and A13 interact with TonB residues V225, V226, L229, and K231 on one side and with TonB Q160 on the other (20).

bioRxiv preprint doi: https://doi.org/10.1101/2021.12.08.471779; this version posted December 8, 2021. The copyright holder for this preprint (which was not certified by peer review) is the author/funder. All rights reserved. No reuse allowed without permission.

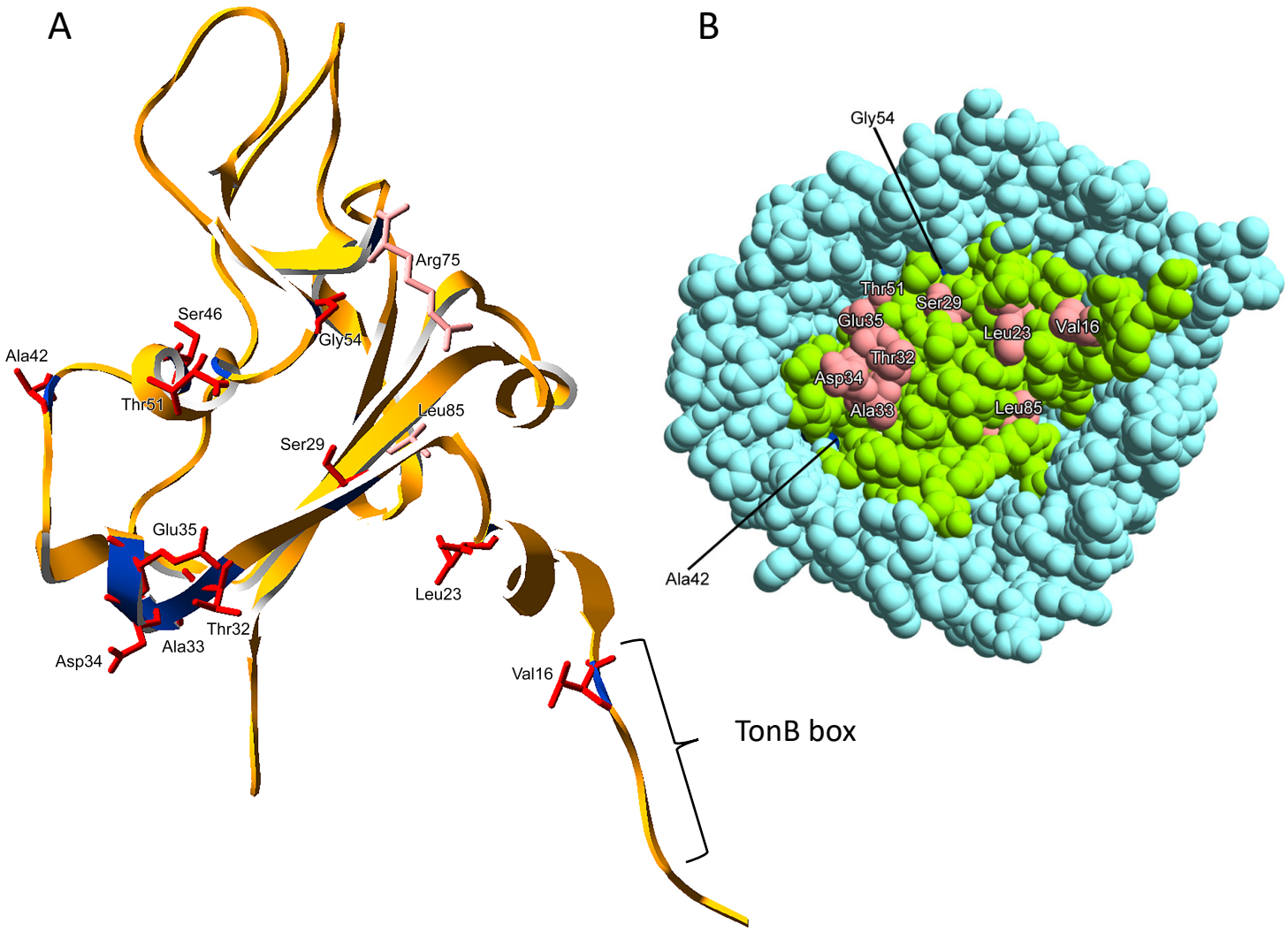


**Figure 9: The FepA cork, residues 1-85. (A)** Ribbon diagram of the FepA cork showing residues 1-85 in the mechanically weak segment of the FepA cork that were chosen for Cys substitution and *in vivo* disulfide crosslinking. The external surface of the cork is at the top, the periplasmic surface is at the bottom. The TonB box is indicated. Red residues formed crosslinks; pink residues did not. **(B)** Space filling model of the periplasmic surface of FepA, showing periplasmic accessibility

bioRxiv preprint doi: https://doi.org/10.1101/2021.12.08.471779; this version posted December 8, 2021. The copyright holder for this preprint (which was not certified by peer review) is the author/funder. All rights reserved. No reuse allowed without permission.

of the residues labelled in (A). The FepA barrel is light blue; the FepA cork is light green; the periplasmically accessible residues tested are shown in pink. T51 is partially accessible; Gly54 and Ala42 (dark blue) are barely visible; Ser46 is completely buried. The crystal structure was solved by Buchanan et al. (60).

bioRxiv preprint doi: https://doi.org/10.1101/2021.12.08.471779; this version posted December 8, 2021. The copyright holder for this preprint (which was not certified by peer review) is the author/funder. All rights reserved. No reuse allowed without permission.

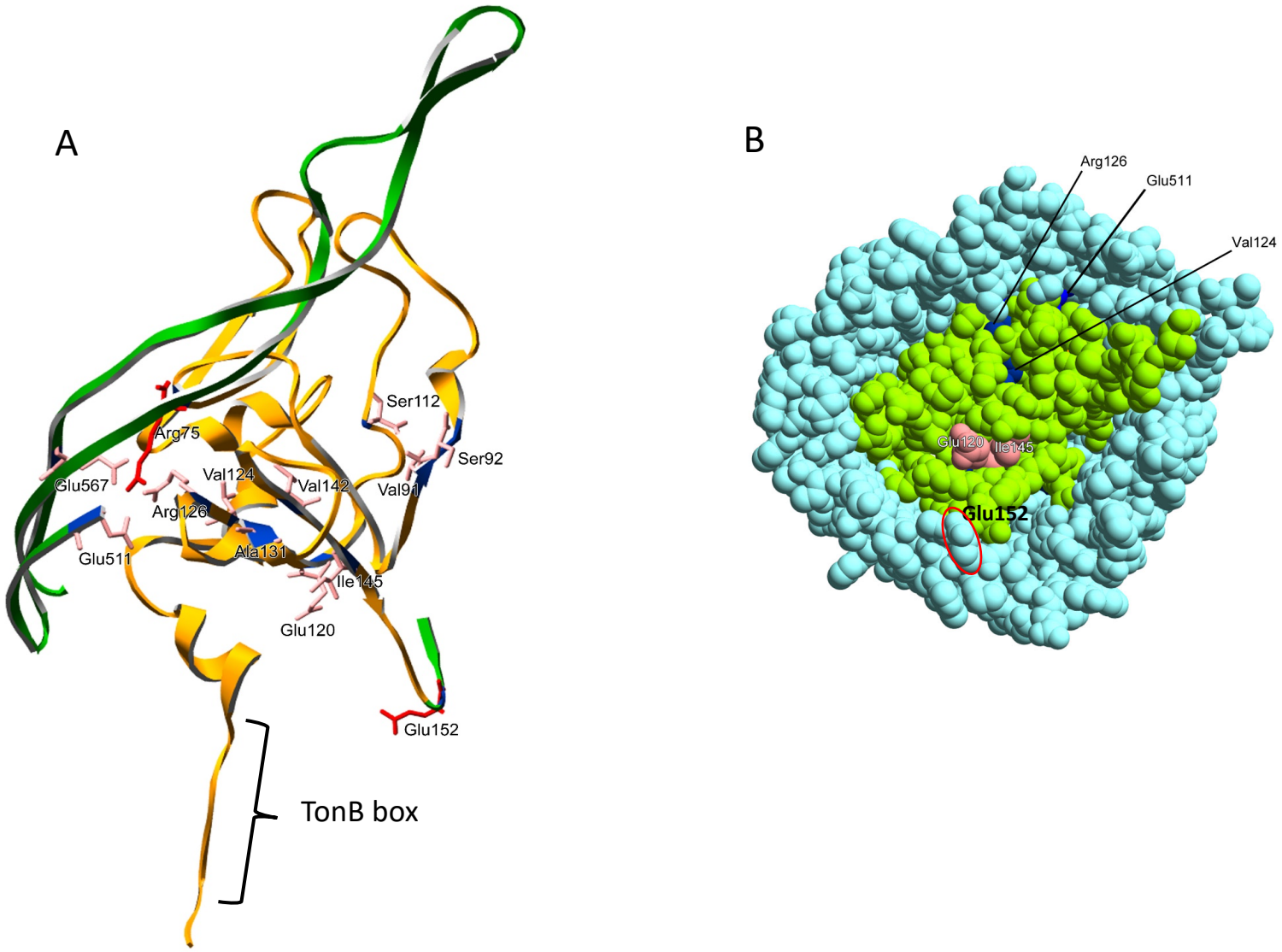


**Figure 10. The FepA cork, residues 75-152. (A)** Ribbon diagram of the FepA cork showing residues 75-152, a mechanically recalcitrant segment of the cork, that were chosen for Cys substitution and *in vivo* disulfide crosslinking. The external surface of the cork is at the top, the periplasmic surface is at the bottom. The TonB box is indicated. Red residues formed crosslinks; pink residues did not.

bioRxiv preprint doi: https://doi.org/10.1101/2021.12.08.471779; this version posted December 8, 2021. The copyright holder for this preprint (which was not certified by peer review) is the author/funder. All rights reserved. No reuse allowed without permission.

Arg75 should be pink instead of red. Portions of the FepA barrel (dark green) show residues Glu511 and Glu567 which together with cork residues Arg75 and Arg126 form the lock region (54). **(B)** Space filling model of the periplasmic surface of FepA, showing periplasmic accessibility of the residues labelled in (A). The FepA barrel is blue; the FepA cork is light green; periplasmically accessible residues are shown in pink. Semi-accessible residues are dark blue. Glu 152 is circled in red. The crystal structure was solved by Buchanan et al. (60).

bioRxiv preprint doi: https://doi.org/10.1101/2021.12.08.471779; this version posted December 8, 2021. The copyright holder for this preprint (which was not certified by peer review) is the author/funder. All rights reserved. No reuse allowed without permission.

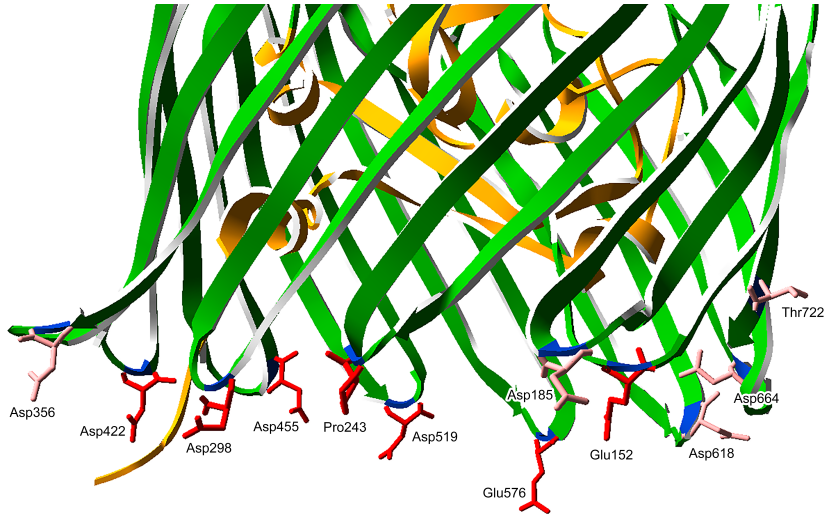


**Figure 11. The FepA barrel β-strand turns.** Ribbon diagram of the FepA β-strand turns chosen for Cys substitution and *in vivo* disulfide crosslinking. Beta strands of the barrel are colored dark green. Red residues formed crosslinks; pink residues did not. The crystal structure was solved by Buchanan et al. (60).

bioRxiv preprint doi: https://doi.org/10.1101/2021.12.08.471779; this version posted December 8, 2021. The copyright holder for this preprint (which was not certified by peer review) is the author/funder. All rights reserved. No reuse allowed without permission.

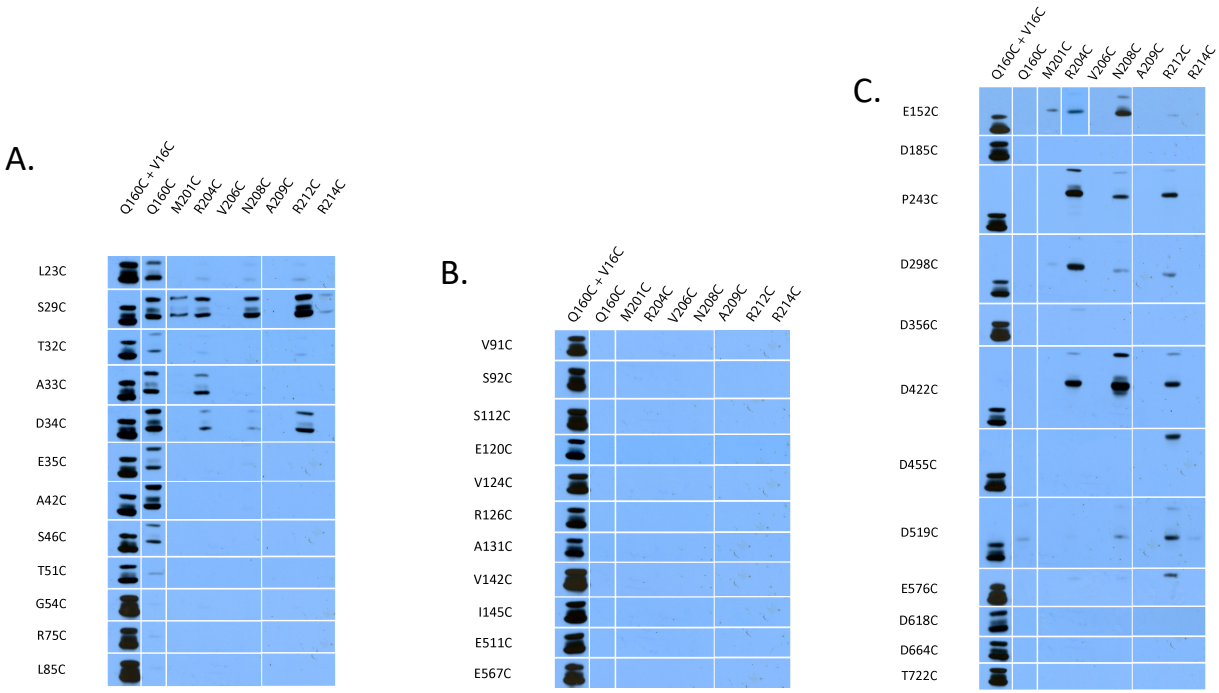


1408

1409

1410 **Fig. 12 The composite comparison of *in vivo* TonB-FepA disulfide**

1411 **interactions identifies the interactive core of the TonB amphipathic helix as its**

1412 **hydrophilic face. (A)** TonB Cys substitutions paired with FepA Cys substitutions

1413 from the mechanically weak region of the FepA cork (residues 1-70) as well as

1414 R75C and L85C from the transition between mechanically weak and mechanically

1415 recalcitrant domains. R75 is considered a part of the "lock region". **(B)** TonB Cys

1416 substitutions paired with FepA Cys substitutions from the mechanically recalcitrant

1417 region of the FepA cork (residues 91-145) and the FepA "lock region" (residues

1418 R126, E511C and E567C). **(C)** TonB Cys substitutions paired with FepA Cys

1419 substitutions located in barrel β-strand turns as well as FepA E152C located at the

bioRxiv preprint doi: https://doi.org/10.1101/2021.12.08.471779; this version posted December 8, 2021. The copyright holder for this preprint (which was not certified by peer review) is the author/funder. All rights reserved. No reuse allowed without permission.

transition between the FepA cork and barrel. TonB Cys substitutions are indicated across the top of the immunoblots. FepA Cys substitutions are indicated along the left side of each composite. TonB-FepA disulfide-crosslinked complexes were visualized in strain KP1491[W3110 Δ*fepA,* Δ(*tonB,P14*)*::kan*]. Composite immunoblots of non-reducing SDS polyacrylamide gels with anti-TonB monoclonal antibody are shown. Since not all experiments were performed on the same immunoblot, exposures for this composite summary were chosen based on matching the Q160C + V16C standards among immunoblots (left-most lanes in A, B, and C).

bioRxiv preprint doi: https://doi.org/10.1101/2021.12.08.471779; this version posted December 8, 2021. The copyright holder for this preprint (which was not certified by peer review) is the author/funder. All rights reserved. No reuse allowed without permission.

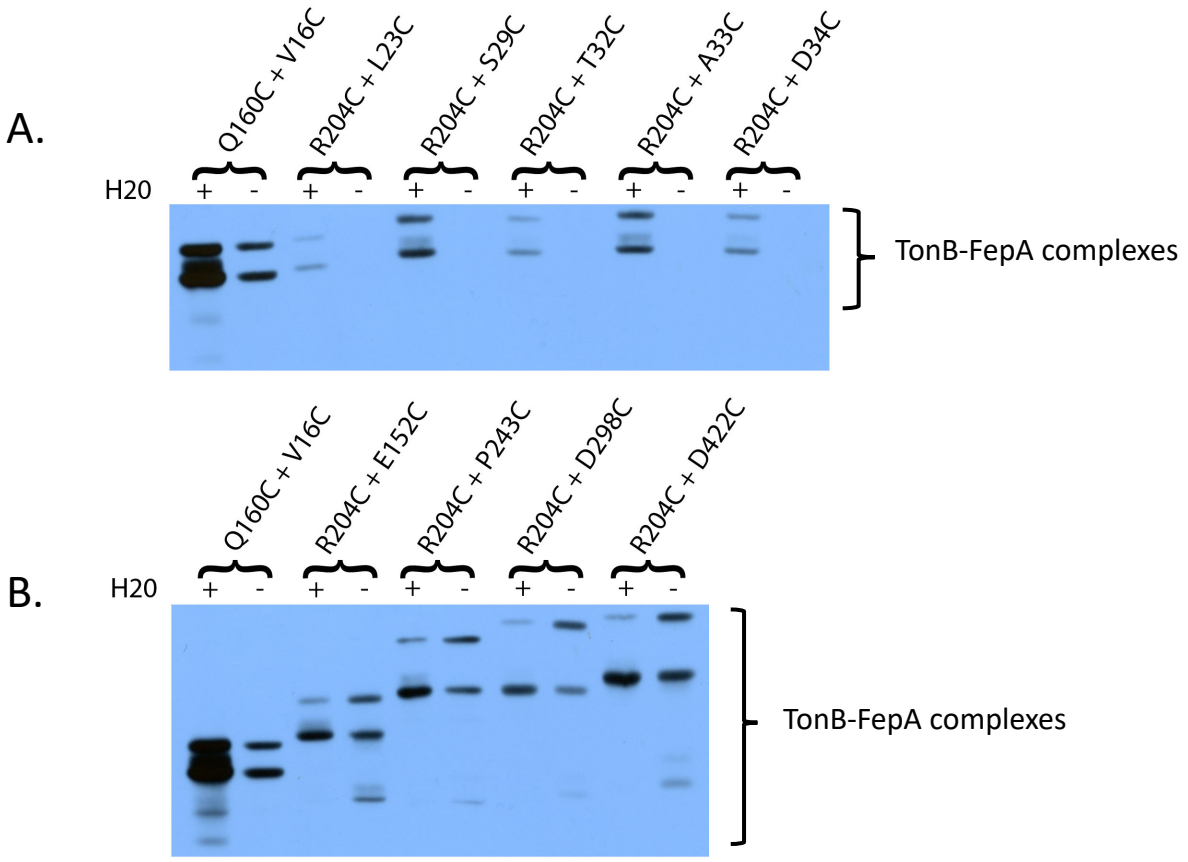


1431

1432

1433 **Figure 13: *In vivo*, TonB R204C makes both functionally important and**

1434 **functionally unimportant disulfide crosslinks with FepA Cys substitutions.**

1435 TonB Cys substitution + FepA Cys substitution combinations are indicated at the

1436 top of each set of lanes. H20 (+) indicates the presence of the wild-type H20 allele

1437 in the TonB transmembrane domain. (-) indicates the presence of the inactivating

1438 H20A mutation. **(A)** The presence of the TonB H20A mutation significantly

1439 reduced disulfide crosslinking by FepA early cork Cys substitutions (depicted in

1440 Fig. 9). **B).** The H20A mutation has little effect on the overall abundance of

bioRxiv preprint doi: https://doi.org/10.1101/2021.12.08.471779; this version posted December 8, 2021. The copyright holder for this preprint (which was not certified by peer review) is the author/funder. All rights reserved. No reuse allowed without permission.

1441 R204C-mediated disulfide crosslinks at the cork-barrel interface, specifically FepA
1442 E152C (depicted in Fig. 10) or the barrel turns, where they occurred (depicted in
1443 Fig. 11). The TonB Q160C-FepA V16C pair was used as a standard for
1444 comparison of relative levels (far left lanes in A. and B.). TonB-FepA disulfide-
1445 crosslinked complexes were visualized in strain KP1491[W3110 Δ*fepA,*
1446 Δ(*tonB,P14*)*::kan*]. Immunoblots of non-reducing SDS polyacrylamide gels with
1447 anti-TonB monoclonal antibody are shown. Monomer TonB levels for all samples
1448 in these immunoblots were at or near chromosomal levels (data not shown).
1449
1450

bioRxiv preprint doi: https://doi.org/10.1101/2021.12.08.471779; this version posted December 8, 2021. The copyright holder for this preprint (which was not certified by peer review) is the author/funder. All rights reserved. No reuse allowed without permission.

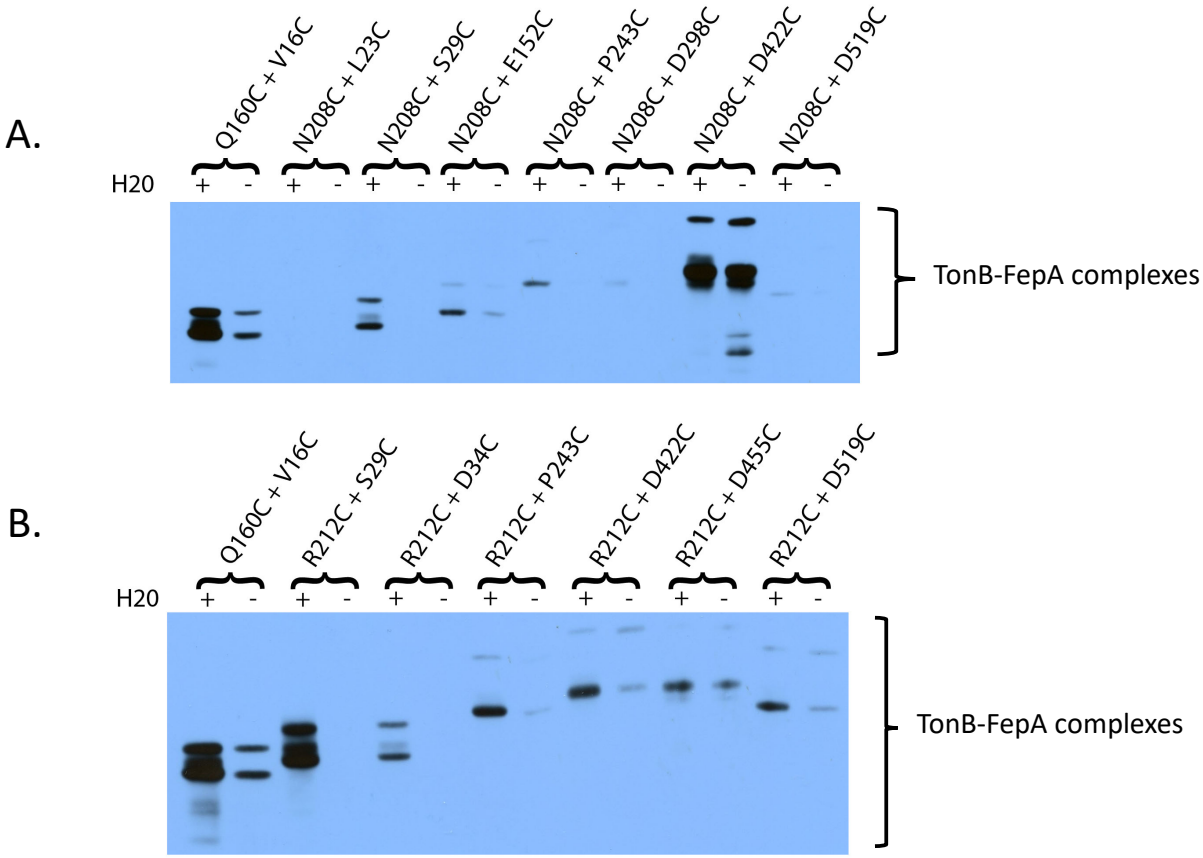


**Figure 14:** ***In vivo*****, TonB N208C and TonB R212C make both functionally important and functionally unimportant disulfide crosslinks with FepA Cys substitutions.** TonB Cys substitution + FepA Cys substitution combinations are indicated at the top of each set of lanes. H20 (+) indicates the presence of the wild-type H20 allele in the TonB transmembrane domain. (-) indicates the presence of the inactivating H20A mutation. **(A)** The presence of the TonB H20A mutation generally reduced disulfide crosslinking by TonB N208C. The notable exception was the very abundant crosslink with D422C, located in a FepA barrel turn

bioRxiv preprint doi: https://doi.org/10.1101/2021.12.08.471779; this version posted December 8, 2021. The copyright holder for this preprint (which was not certified by peer review) is the author/funder. All rights reserved. No reuse allowed without permission.

(depicted in Fig. 11). This interaction was impervious to the presence of the H20A mutation. **(B)** Most notably, TonB R212C makes a very abundant, H20-specific, crosslink with FepA S29C (depicted in Fig. 9). It also makes H20-specific complexes with some of the FepA Cys substitutions in the barrel turns (depicted in Fig. 11). The TonB Q160C-FepA V16C pair was used as a standard (far left lanes in A. and B.). TonB-FepA disulfide-crosslinked complexes were visualized in strain KP1491[W3110 Δ*fepA,* Δ(*tonB,P14*)*::kan*]. Immunoblots of non-reducing SDS polyacrylamide gels with anti-TonB monoclonal antibody are shown. Monomer TonB levels for all samples in these immunoblots were at or near chromosomal levels (data not shown).

bioRxiv preprint doi: https://doi.org/10.1101/2021.12.08.471779; this version posted December 8, 2021. The copyright holder for this preprint (which was not certified by peer review) is the author/funder. All rights reserved. No reuse allowed without permission.

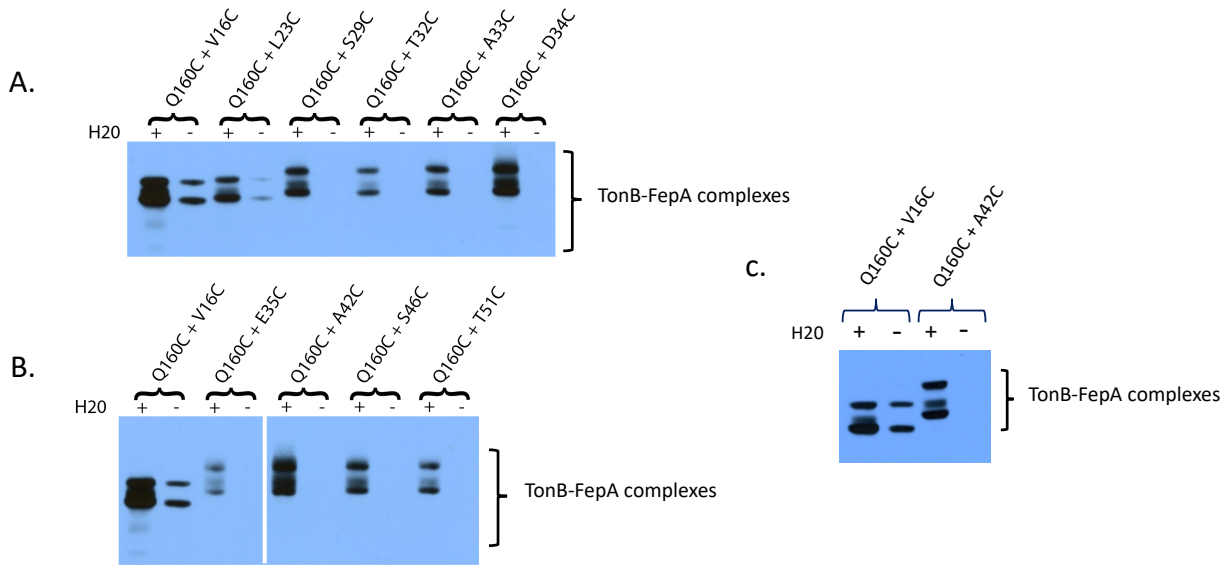


1474

1475

1476 **Figure 15: *In vivo*, TonB Q160C makes several functionally important**

1477 **disulfide crosslinks within the mechanically weak segment of the FepA cork,**

1478 **including with buried residues (depicted in Fig. 9).** TonB Cys substitution +

1479 FepA Cys substitution combinations are indicated at the top of each lane. H20 (+)

1480 indicates the presence of the wild-type H20 allele in the TonB transmembrane

1481 domain. (-) indicates the presence of the inactivating H20A mutation. **(A)** TonB

1482 Q160C made complexes with several FepA substitutions, all of which were

1483 prevented by the TonB H20A mutation. Notably the complex with FepA D34 was

1484 of nearly equal abundance to the standard TonB Q160C-FepA V16C pair; unlike

1485 that standard, it was entirely prevented by the presence of the TonB H20A

1486 mutation. **(B)** TonB Q160C makes a complex with buried residue FepA A42C of

1487 nearly equal abundance to the standard TonB Q160C-FepA V16C pair; it was

bioRxiv preprint doi: https://doi.org/10.1101/2021.12.08.471779; this version posted December 8, 2021. The copyright holder for this preprint (which was not certified by peer review) is the author/funder. All rights reserved. No reuse allowed without permission.

entirely prevented by the presence of the TonB H20A mutation. For this composite immunoblot, the exposure on the right was chosen based on matching it to the same intensity as the Q160 + V16C standard shown in the left panel. **(C)** Direct comparison of Q160C complexes with FepA V16C and FepA A42C on the same immunoblot and with a shorter exposure. TonB-FepA disulfide-crosslinked complexes were visualized in strain KP1491[W3110 Δ*fepA,* Δ(*tonB,P14*)*::kan*]. Immunoblots of non-reducing SDS polyacrylamide gels with anti-TonB monoclonal antibody are shown. Monomer TonB levels for all samples in these immunoblots were at or near chromosomal levels (data not shown).

bioRxiv preprint doi: https://doi.org/10.1101/2021.12.08.471779; this version posted December 8, 2021. The copyright holder for this preprint (which was not certified by peer review) is the author/funder. All rights reserved. No reuse allowed without permission.

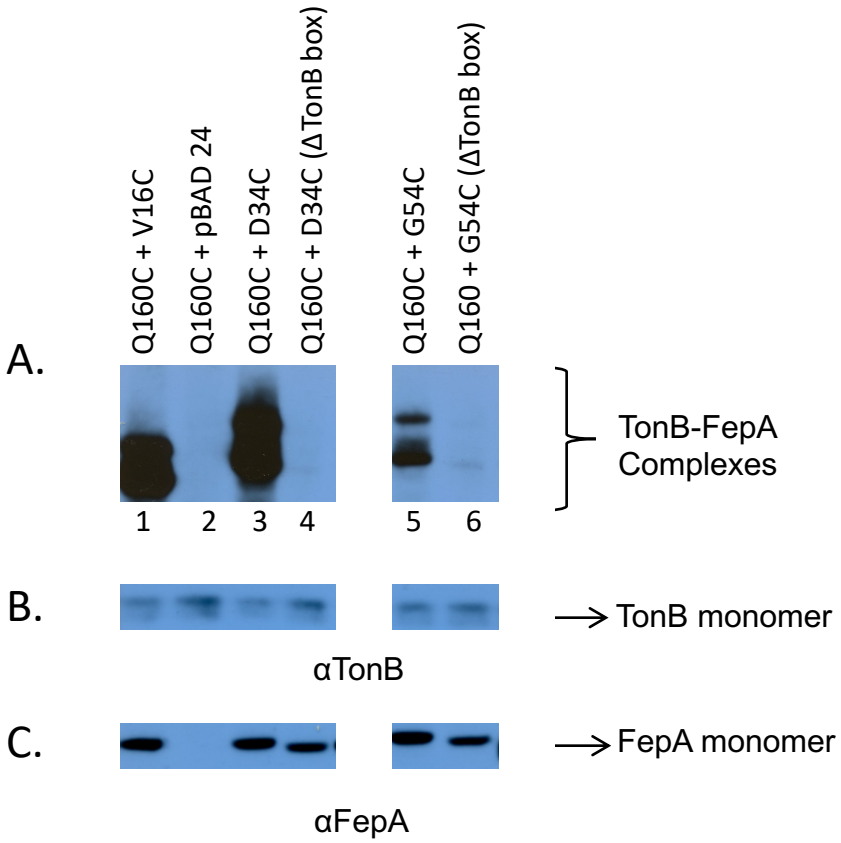


**Figure 16. Deletion of the FepA TonB box prevents *in vivo* disulfide complex formation by TonB Q160C. (A)** TonB-FepA disulfide-crosslinked complexes visualized in strain KP1491[W3110 Δ*fepA,* Δ(*tonB,P14*)*::kan*] by immunoblots of non-reducing SDS polyacrylamide gels with anti-TonB monoclonal antibody. pBAD24 is the vector into which *fepA* variants were cloned. **(B)** Monomer levels of TonB from the same samples as A), visualized by anti-TonB monoclonal antibody. **(C)** Monomer levels of FepA from same samples as A.), visualized by

bioRxiv preprint doi: https://doi.org/10.1101/2021.12.08.471779; this version posted December 8, 2021. The copyright holder for this preprint (which was not certified by peer review) is the author/funder. All rights reserved. No reuse allowed without permission.

anti-FepA polyclonal antibody. All lanes are from the same immunoblot with a center lane masked.

bioRxiv preprint doi: https://doi.org/10.1101/2021.12.08.471779; this version posted December 8, 2021. The copyright holder for this preprint (which was not certified by peer review) is the author/funder. All rights reserved. No reuse allowed without permission.

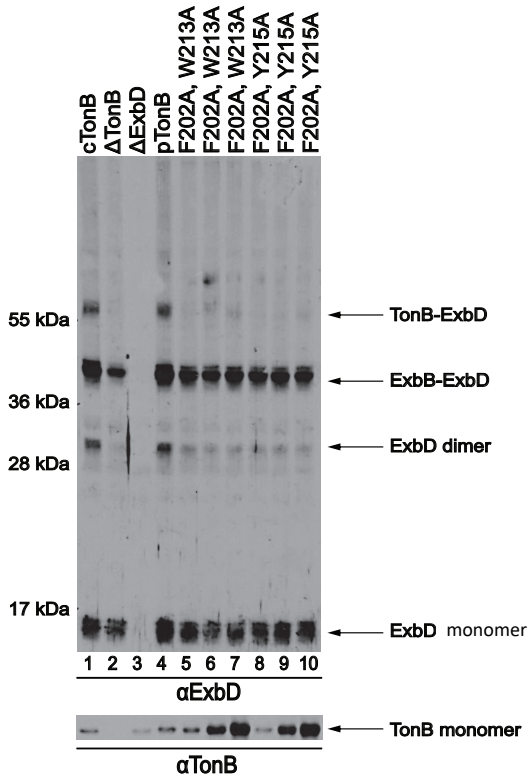


**Figure 17. TonB F202A, W213A does not form the TonB-ExbD heterodimer.** **Upper:** Immunoblot with anti-ExbD antibodies of formaldehyde crosslinked samples. Lane 1, W3110 expressing chromosomally encoded TonB (cTonB); Lane 2, KP1344 [W3110 Δ(*tonB, P14)::blaM*]; Lane 3 RA1021 (W3110 Δ*exbD*); Lane 4, plasmid-encoded TonB (pKP442) with 0.001% arabinose; Lane 5, pKP531 (pKP442 TonB with F202A, W213A double mutations) with 0.002% arabinose; Lane 6, pKP531 with 0.005% arabinose; Lane 7, pKP531 with 0.01% arabinose; Lane 8, pKP532 (pKP442 TonB with F202A, W215A double mutations) with 0.002% arabinose; Lane 9, pKP532 with 0.005% arabinose; Lane 10, pKP532 with 0.01% arabinose. **Lower:** Corresponding steady state levels of TonB from the

bioRxiv preprint doi: https://doi.org/10.1101/2021.12.08.471779; this version posted December 8, 2021. The copyright holder for this preprint (which was not certified by peer review) is the author/funder. All rights reserved. No reuse allowed without permission.

1523 samples above are shown. For pKP531 and pKP532, note the increase in TonB

1524 expression with increasing addition of the inducer, arabinose.

1525

1526

bioRxiv preprint doi: https://doi.org/10.1101/2021.12.08.471779; this version posted December 8, 2021. The copyright holder for this preprint (which was not certified by peer review) is the author/funder. All rights reserved. No reuse allowed without permission.

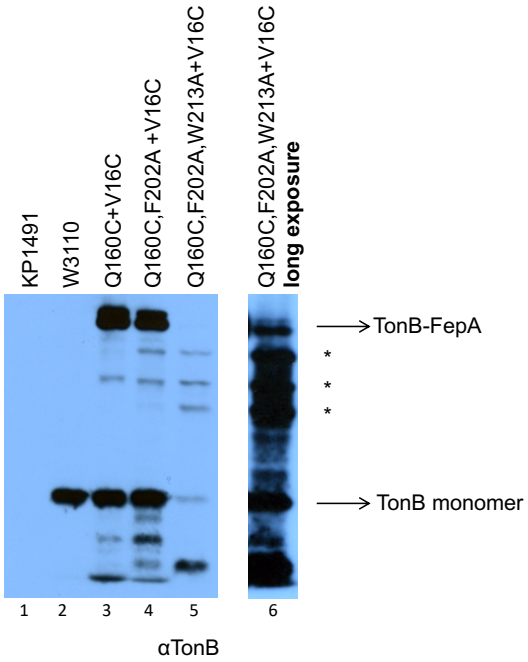


**Figure 18. Inactivation of the TonB carboxy terminus appears to divert TonB Q160C down a path to triplet homodimer formation.** Lane 1, KP1491 [W3110 Δ*fepA,* Δ(*tonB,P14*)*::kan*]: the parent strain used in all these studies. Lane 2, W3110: the wild-type strain showing the steady state level of chromosomally encoded TonB. Lane 3, TonB Q160C in combination with FepA V16C. Lane 4, TonB Q160C with the additional F202A substitution in combination with FepA V16C. Lane 5, TonB Q160C in combination with additional F202A and W213A substitutions in combination with FepA V16C. Lane 6, long exposure of lane 5 to reveal relative levels of TonB-FepA and triplet homodimer complexes. Positions of TonB monomer and TonB-FepA complexes are indicated on the right. Potential triplet homodimers are indicated by asterisks (*). Immunoblots of non-reducing

bioRxiv preprint doi: https://doi.org/10.1101/2021.12.08.471779; this version posted December 8, 2021. The copyright holder for this preprint (which was not certified by peer review) is the author/funder. All rights reserved. No reuse allowed without permission.

SDS polyacrylamide gels developed with monoclonal anti-TonB antibody are shown.